Elastic and electric properties of North Sea Chalk

Olsen, Casper; Fabricius, Ida Lykke

Publication date:
2007

Document Version
Publisher's PDF, also known as Version of record

DTU

Elastic and electric properties of North Sea Chalk

Casper Olsen

INSTITUTE OF ENVIRONMENT & RESOURCES

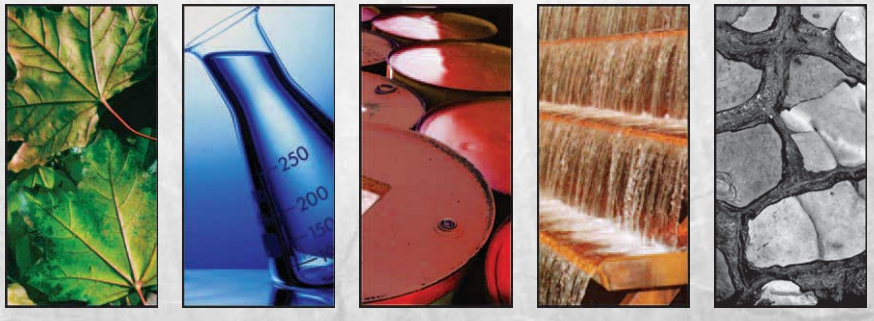

Elastic and electric properties of North Sea Chalk

Casper Olsen

Ph.D. Thesis

August 2007

Institute of Environment & Resources

Technical University of Denmark

Elastic and electric properties of North Sea Chalk.

Cover: Torben Dolin & Julie Camilla Middleton
Printed by: Vester Kopi, DTU
Institute of Environment & Resources
ISBN 978-87-91855-41-2

The thesis will be available as a pdf-file for downloading from the institute homepage on: www.er.dtu.dk

Institute of Environment & Resources
Library
Bygningstorvet, Building 115,
Technical University of Denmark
DK-2800 Kgs. Lyngby

Phone:
Direct: (+45) 45 25 16 10
(+45) 45 25 16 00
Fax: (+45) 45 93 28 50
E-mail: library@er.dtu.dk

Preface

This Ph.D. thesis entitled "Elastic and electric properties of North Sea chalk" is based on research carried out at Institute of Environment and Resources, Technical University of Denmark (DTU) with associate professor Ida Lykke Fabricius as principal supervisor. The project was financed by DTU. The experimental work in this thesis was carried out at GEO, Danish Geotechnical Institute in co-operation with Helle Foged Christensen. During the Ph.D. study I stayed three month with Stanford Rock Physics and Borehole Geophysics Project (SRB), Department of Geophysics where I worked together with research associate Manika Prasad. This thesis comprises a report, three manuscripts submitted to the journal *Geophysics*, four conference abstract and two related co-authored papers.

- Olsen, C., K. Hedegaard, I.L. Fabricius, and M. Prasad, Prediction of Biot's coefficient from rock physical modeling of North Sea chalk: Submitted to Geophysics.
- Olsen, C., H.F. Christensen, and I.L. Fabricius, Static and dynamic Young's modulus of chalk from the North Sea: Submitted to Geophysics.
- Olsen, C., T. Hongdul, and I. L. Fabricius, Prediction of Archie's cementation factor from specific surface or from porosity and permeability: Submitted to Geophysics.
- Olsen, C., I. L. Fabricius, A. Krogsbøll, M. Prasad, 2004, Static and Dynamic Young's Modulus of Marly Chalk from the North Sea: 66th Conference and Exhibition, EAGE.
- Olsen, C., I. L. Fabricius, A. Krogsbøll, M. Prasad, 2004, Static and dynamic Young's Modulus for Lower Cretaceous chalk. A low frequency scenario.: International Conference and Exhibition, AAPG.
- Olsen, C., K. Hedegaard, I. L. Fabricius, M. Prasad, 2005, Modelling elastic moduli and cementation of North Sea chalk: 67th Conference & Exhibition, EAGE.
- Olsen, C., and I. L. Fabricius, 2006, Static and dynamic Young's modulus of North Sea chalk: 76th Annual International Meeting, SEG, Expanded abstract, 1918-1922.

Publications co-authored related to this study:

- Fabricius, I.L., C. Olsen, and M. Prasad, 2005, Log interpretation of marly chalk, the lower Cretaceous Valdemar field Danish North Sea: Application of iso-frame and pseudo water-film concepts: The Leading Edge, **May 2005**, 496-505.
- Prasad, M., I.L. Fabricius, and C. Olsen, 2005, Rock physics and statistical well log analysis in marly chalk: The Leading Edge, **May 2005**, 491-495.

The papers are not included in this www-version but can be obtained from the library at the Institute of Environment and Resources, Bygningstorvet, Building 115, Technical University of Denmark Dk-2800 Kgs. Lyngby, (library@er.dtu.dk).

Abstract

This Ph.D. thesis consists of a report, three manuscripts submitted to the Journal "*Geophysics"*, four conference abstracts and two related studies. The Ph.D. study has the title "Elastic and electric properties of North Sea Chalk" and it is divided into three main parts.

The first part of the study is about modeling elastic moduli and cementation of North Sea chalk. This part of the study was based on laboratory measurements of acoustic velocities. Biot's coefficient for chalk was discussed versus another measure of cementation, the specific surface of chalk. Biot's coefficient is in agreement with the specific surface and Biot's coefficient was used as a physical measure of degree of cementation or pore space compressibility. Four different effective medium models with different approaches were used to model chalk; the Iso-Frame model, the bounding average model (BAM), Berryman's self-consistent model and Dvorkin's cemented sand model. The self-consistent model is used with two different combinations of aspect ratio, the first combination defines aspect ratio for the grains and the pores to be equal and the other combination defines aspect ratio for the grains to be constant close to one and the aspect ratio of the pores varies. Each of the models contains one free parameter, this parameter is related to pore space compressibility and it was compared to Biot's coefficient. It was analyzed how well the models predicts two different elastic moduli for dry and water-saturated chalk based on the same assumptions for the rock. It was also discussed how well the models predicts Biot's coefficient based on P-wave velocity and density for water-saturated chalk. The Iso-Frame model and the BAM model are in general more consistent than the self-consistent model by Berryman when both dry and water-saturated chalk is modeled. The cemented sand model is only consistent between two moduli for the softest chalk samples and it is only applicable to dry rock. For the Iso-Frame model, the BAM model and the cemented sand model the free parameter in the model is in agreement with Biot's coefficient. For Berryman's self-consistent model the free parameter is only in agreement with Biot's coefficient for water-saturated chalk when the aspect ratio for the pores and the grains are equal. The Iso-Frame model and the BAM model predicts Biot's coefficient based on P-wave velocity and density for water-saturated chalk better than the self-consistent model by Berryman. The cemented sand is not used for prediction of Biot's coefficient based on P-wave velocity and density of water-saturated chalk because it is only applicable to dry rock.

The second part of the study is concerned with relating static and dynamic Young's modulus for both stiff cemented chalk and soft chalk with a minor degree of cementation. For the stiff cemented chalk the samples deformed close to linear elastic during static loading and it was in this case possible to compare static and dynamic Young's modulus directly. For dry chalk the static and dynamic Young's modulus are equal, in this case no influence from a difference in frequency or strain amplitude between the static and dynamic measurements was observed. Based on the results from the dry chalk it was possible to discuss influence of pore fluid on a possible difference

between static and dynamic Young's modulus for water-saturated chalk. For water-saturated chalk a difference between static and dynamic Young's modulus was observed and the difference between static and dynamic Young's modulus may be caused both by a difference in drainage conditions between static and dynamic measurements and a difference in frequency between static and dynamic measurements. It was in this study not possible to quantify the influence from a difference in drainage conditions based on experiments. Static Young's modulus was obtained with two different methods both strain gauge and LVDT (Linear Voltage Displacement Transducer). Static Young's modulus based on strain gauge is related to dynamic Young's modulus but static Young's modulus based on LVDT is not related to dynamic Young's modulus. The influence from the experimental setup on the LVDT measurements is so large that it is not possible accurately to measure small strains for stiff materials like chalk for small stresses with LVDT.

For a set of less cemented samples from Lower Cretaceous chalk formations in the North Sea static and dynamic Young's modulus was compared. For these samples a significant non-elastic deformation occurred during static loading. In this study a model was developed to relate static and dynamic Young's modulus when non-elastic deformation occurs during static loading. In this model the non-elastic deformation during static loading is described with a non-elastic Young's modulus and this non-elastic modulus can be obtained from the static loading curve.

In the third part of the study it was analyzed how Archie's cementation factor depends on other physical properties for a reservoir rock. The cementation factor was measured in the laboratory on North Sea chalk samples and published cementation factors for sandstones were also used in the study. The cementation factor for chalk depends on specific surface with respect to bulk volume of chalk. For both chalk and sandstone it was discussed if it is possible to predict cementation factor from a calculated effective specific surface through Kozeny's equation and porosity and permeability. It was also discussed if it is possible to relate electric properties and acoustic properties for chalk by relating Archie's cementation factor to Biot's coefficient. Both Biot's coefficient and cementation factor are dependent on degree of cementation. The cementation factor depends primarily on the smoothness of the grains in the sediment and Biot's coefficient depends primarily on stiffness of the grain contacts. The relationship between cementation factor and Biot's coefficient is vague due to a variation in the content of fine grained silica. Silica has a significant influence on specific surface of chalk and the cementation factor but it does not have a significant effect on grain contact stiffness and Biot's coefficient.

Dansk resumé

Denne Ph.D. afhandling består af en sammenfatning, tre manuskripter submitted til tidskriftet *Geophysics*, fire konference abstracts og to relaterede artikler. Ph.D. studiet har titlen ”Elastiske og elektriske egenskaber for Nordsø kalk” og studiet er delt i tre emner.

Den første del af studiet omhandler modellering af elastiske moduler og cementering af Nordsø kalk. Denne del af studiet er baseret på laboratorie målinger af akustiske hastigheder. Biots koefficient diskuteres versus et andet mål for cementering, den specifikke overflade. Biots koefficient er i overensstemmelse med den specifikke overflade og Biots koefficient bruges som et mål for cementering eller pore kompressibilitet. Fire forskellige fysiske modeller med hvert sin tilgang til modelering analyseres: Iso-Frame model, bounding avaerage model (BAM), Berryman self-consistent model, og Dvorkins cemented sand model. Self-consistent modellen anvendes med to forskellige kombinationer af aspect ratio, i den første kombination defineres aspect ratio for korn og pore til at være lige store og i den anden kombination defines aspect ratio for korn til at være konstant tæt på en og aspect ratio for pore varierer. Hver af modellerne indeholder en fri parameter, denne frie parameter er et mål for pore kompresibilitet, og denne frie parameter diskuteres i forhold til Biots koefficient. Det analyseres om modellerne kan modellere to uafhængige elastiske moduler konsistent for tør og vandmættet kalk baseret på de samme antagelser for kalken. Det analyseres også om de forskellige modeller kan forudsige Biots koefficient ud fra P-bølge hastighed og densitet for vandmættet kalk. Iso-Frame modellen og BAM modellen er generelt mere konsistente end Berrymans self-consistent model, når både tør og vandmættet kalk modeleres. Cemented sand model er kun konsistent mellem to moduler for den blødeste kalk, og den kan kun modellere tørre bjergarter. For Iso-Frame modellen, BAM modellen, og cemented sand model er den frie parameter i overensstemmelse med Biots koefficient. For self-consistent modellen er den frie parameter kun i overensstemmelse med Biots koefficient for vandmættet kalk, når aspect ratio for pore og korn er lige store. Iso-Frame modellen og BAM modellen forudsiger Biots koefficient bedre baseret på P-bølge hastighed og densistet for vandmættet kalk end self-consistent modellen. Cemented sand model bruges ikke til at forudsige Biots koefficient basseret på P-bølge hastighed og densistet for vandmættet kalk, fordi denne model kun kan bruges for tørre bjergarter.

Den anden del af studiet omhandler sammenligning af statisk og dynamisk Young’s modul for både cementeret stiv kalk og mindre cementeret blød kalk. Den stive kalk deformerer næsten lineært elastisk under statisk deformation, og det er muligt at sammenligne statisk of dynamisk Young’s modul direkte. For tør kalk er det statiske og dynamiske modul ens, forskellen i frekvensen og tøjningens størrelse i de to forskellige målemetoder har ikke nogen indflydelse på modulet, der måles. Baseret på resultatet for de tørre prøver, kan indflydelsen fra porevæsken på en mulig forskel mellem statisk og dynamisk modul diskuteres for de vandmættede prøver. Der blev observeret en forskel

mellem dynamisk Youngs modul og statisk Youngs modul for vandmættet kalk, og denne forskel mellem det statiske og dynamiske modul skyldes forskellen i dræningstilstanden og forskellen i frekvensen mellem den statiske og dynamiske målemetode. Det var ikke muligt i dette studie at kvantificere indflydelsen fra forskellen i dræning mellem statisk og dynamisk måling eksperimentielt. Det statiske modul blev målt med to forskellige metoder, strain gauge og LVDT (Linear Voltage Displacement Transducer). Det statiske modul målt med strain gauge er sammenligneligt med det dynamiske modul, men det statiske modul målt med LVDT er ikke sammenligneligt med det dynamiske modul. Indflydelse på måleresultaterne fra forsøgsopstillingen er så stor for LVDT, at det ikke er muligt at måle deformationer nøjagtigt nok med LVDT for små deformationer ved lave mekaniske spændinger.

Statisk og dynamisk Youngs modul blev også sammenlignet baseret på mindre cementerede prøver fra Nedre Kridt formationen i Nordsøen. For disse prøver blev der observeret en signifikant ikke-elastisk deformation under den statiske deformation. I denne del af studiet blev det diskuteret, hvordan statisk og dynamisk Young's modul forholder sig til hinanden, når en signifikant ikke-elastisk deformation forekommer under statisk deformation. Der blev foreslået en model, der sammenkæder statisk og dynamisk Youngs modul, når ikke-elastisk deformation forekommer i løbet af statisk deformation. I denne model beskrives den ikke-elastiske deformation med et ikke-elastisk modul, der kan bestemmes ud fra arbejdskurven fra den statiske måling.

I den tredie del af studiet analyseres det hvilke andre fysike egenskaber Archies cementeringsfaktor afhænger af for en reservoir bjergart. Cementeringsfaktoren blev målt i laboratorium for Nordsø kalk, og publiserede cementeringsfaktorer for sandsten blev også inddraget i studiet. Cementeringsfaktoren for kalk afhænger af den specifikke overflade for kalk normeret i forhold til bulk volumen af prøven. For både Nordsø kalk og sandsten diskuteres det, om det er muligt at forudsige cementeringsfaktoren ud fra den effektive specifikke overflade beregnet ud fra Kozenys ligning og porositet og permeabilitet. Det diskuteres også, om det er muligt at sammenkæde elektriske egenskaber og akustiske egenskaber for kalk ved at sammenligne Archies cementeringsfaktor med Biots koefficient. Både Archies cementeringsfaktor og Biots koefficient afhænger af graden af cementering. Cementeringsfaktoren afhænger primært af formen af kornene, og Biots koefficient afhænger primært af stivheden af kornkontakterne. Den sammenhæng, der blev fundet mellem cementeringsfaktoren og Biots koefficient, er uklar på grund af et varierende indhold af finkornet kiesel i kalken. Kiesel har en stor indflydelse på den specifikke overflade og cementeringsfaktoren for kalk, men den har ikke nogen særlig indflydelse på kornkontaktstivheden i kalken eller Biots koefficient.

Acknowledgement

I thank my principal supervisor associate professor Ida Lykke Fabricius from Institute of Environment and Resources Technical University of Denmark, DTU for her advises during this Ph.D. study.

I also thank Helle Foged Christensen from GEO, Danish Geotechnical Institute for advises during laboratory work at GEO.

I thank the technical staff at GEO John Christensen, Lars Christensen, Pierre Tjørnehøj, Frederik Ditlevsen and Kathrine Hedegaard for their help during laboratory work.

I also thank Manika Prasad from Stanford Rock Physics and Borehole Geophysics Project (SRB), Department of Geophysics, Stanford University for her interest in my project and for her comments to my work.

I thank associate professor Anette Krogsbøll from BYG-DTU, Technical University of Denmark for her contributions to my work.

I thank senior advisor Niels Spring from GEUS for advises and help with laboratory work.

Mærsk Oil and GAS AS is thanked for providing core material and data for the study.

Ph.D. student Morten Leth Hjuler is also thanked for useful comments to this Ph.D. thesis.

I acknowledge financial support from DTU, DONGs Jubilæumslegat and STVF research grant 26-04-0023.

Kgs. Lyngby June 2007

Casper Olsen

Contents

Enclosures

Manuscripts

Enclosure 1

Olsen, C., K. Hedegaard, I.L. Fabricius, and M. Prasad, Prediction of Biot's coefficient from rock physical modeling of North Sea chalk: Submitted to Geophysics.

Enclosure 2

Olsen, C., H.F. Christensen, and I.L. Fabricius, Static and dynamic Young's modulus of chalk from the North Sea: Submitted to Geophysics.

Enclosure 3

Olsen, C., T. Hongdul, and I. L. Fabricius, Prediction of Archie's cementation factor from specific surface or from porosity and permeability: Submitted to Geophysics.

Conference abstracts

Enclosure 4

Olsen, C., I. L. Fabricius, A. Krogsbøll, M. Prasad, 2004, Static and Dynamic Young's Modulus of Marly Chalk from the North Sea: 66th Conference and Exhibition, EAGE.

Enclosure 5

Olsen, C., I. L. Fabricius, A. Krogsbøll, M. Prasad, 2004, Static and dynamic Young's Modulus for Lower Cretaceous chalk. A low frequency scenario.: International Conference and Exhibition, AAPG.

Enclosure 6

Olsen, C., K. Hedegaard, I. L. Fabricius, M. Prasad, 2005, Modelling elastic moduli and cementation of North Sea chalk: 67th Conference & Exhibition, EAGE.

Enclosure 7

Olsen, C., and I. L. Fabricius, 2006, Static and dynamic Young's modulus of North Sea chalk: 76th Annual International Meeting, SEG, Expanded abstract, 1918-1922.

Related studies

Enclosure 8

Fabricius, I.L., C. Olsen, and M. Prasad, 2005, Log interpretation of marly chalk, the lower Cretaceous Valdemar field Danish North Sea: Application of iso-frame and pseudo water-film concepts: The Leading Edge, **May 2005**, 496-505.

Enclosure 9

Prasad, M., I.L. Fabricius, and C. Olsen, 2005, Rock physics and statistical well log analysis in marly chalk: The Leading Edge, **May 2005**, 491-495.

1. Introduction

When chalk is deposited it consists of loose irregular calcite grains which act as a suspension. After deposition burial diagenesis of the chalk will take place over time and different physical and chemical processes will change the chalk. One process that takes place during burial diagenesis is precipitation of calcite on the surfaces of the grains and in the contact points of the grains. This process is called cementation and it will smoothen the grain surfaces and the grain contacts will become stiffer and the chalk will become a stiffer sediment. In this study cementation will be discussed as a pure physical property that stiffens the grain contacts and smoothens the grain surfaces. It will not be related to geology and burial history of chalk.

Elastic properties of a porous reservoir rock are determined by the porosity, the stiffness properties of the grains and how well the grains are glued together by cement at the grain contacts. Cementation may have a significant influence on acoustic velocities and different properties in rock mechanics. Cementation can also be related to petrophysics when calculations of fluid saturations are performed for a reservoir rock like chalk. The smoothness of the grains may have an influence on properties related to determining fluid saturations.

One physical property that is largely related to cementation of a porous rock is pore space compressibility of the rock because pore space compressibility depends on how well the grain contacts are glued together by cement. Biot's coefficient is related to pore space compressibility therefore Biot's coefficient may be interesting to use as a physical measure of degree of cementation. An analysis of how well Biot's coefficient relates to cementation based on another property that depends on cementation needs to be done. This other property that relates to cementation should not be an elastic property.

Predicting degree of cementation based on acoustic velocities may be of interest because the degree of cementation has a significant influence on different physical properties of chalk. If degree of cementation can be assessed based on acoustic velocities and Biot's coefficient then it may be possible for example to predict weak zones in a reservoir based on acoustic logging data. Biot's coefficient depends on bulk modulus and bulk modulus is dependent on shear wave velocity. Often shear wave velocity is not known for reservoir rocks because shear wave velocity is difficult to obtain. If another measure of cementation can be obtained that only depends on P-wave velocity this parameter could be used to predict degree of cementation if Biot's coefficient can not be determined. This parameter could also be used to predict Biot's coefficient.

In the literature several effective medium models exist that relates acoustic velocities of a rock to elastic properties of the grains in the rock, the pore space and a characteristic property that describes pore space compressibility of the rock (Wang and Nur, 1992). To establish a measure of cementation that only depends on P-wave velocity could be done through one of the effective medium models from the literature and use the property in the effective medium model that describes pore space compressibility as a measure of cementation. A systematic investigation of how well the

measure of pore space compressibility in an effective medium model relates to Biot's coefficient needs to be done. This investigation should also include an analysis of how consistently the model predicts elasticity for chalk. A model is consistent if it can predict two different elastic moduli for a rock based on the same assumptions for the rock.

Static moduli are obtained from rock mechanics experiments in the laboratory and dynamic elastic moduli are obtained from acoustic velocities and density. The static moduli are obtained at a low frequency and with a large strain amplitude, whereas the dynamic moduli are obtained at a high frequency and with a low strain amplitude. Predicting static moduli from dynamic moduli is useful in hydrocarbon production because static moduli are not always available whereas acoustic logging data may be at hand. Static moduli are used to estimate the deformation of a reservoir when the effective stress is changed due to production of hydrocarbons. For reservoir rocks the elastic deformation due to a change in effective stress may be a significant drive mechanism to be included in reservoir simulation. A site specific relationship between static moduli and dynamic moduli is often established for a reservoir based on a few data (Yale and Jamieson, 1994). Static and dynamic moduli are not considered identical when compared in literature and it has been suggested that the difference between static and dynamic modulus is due to differences in frequency and stain amplitude (Wang, 2000). Another problem associated with comparing static and dynamic moduli is related to degree of cementation. For a weak un-cemented rock non-elastic deformation may occur during static loading of the rock but this kind of deformation does not occur when an acoustic wave propagates through a rock. In this case static and dynamic moduli can not be compared directly. A stiff cemented rock may deform close to elastic during static loading and static and dynamic moduli may be comparable but in this case the influence of difference in frequency and strain amplitude between static and dynamic measurements needs to be assessed.
Based on the results in the literature it is not clear how static moduli in general are related to dynamic moduli and further work on relating static and dynamic moduli is necessary.

A central aspect in evaluation of a hydrocarbon reservoir is to calculate fluid saturations and hydrocarbon reserves. Fluid saturation calculation is done based on logging data and an empirical relationship between water saturation, porosity, resistivity of the reservoir rock and resistivity of the pore water introduced by Archie (1942). This relationship also contains an empirical constant; Archie's cementation factor. Archie (1942) postulated that this cementation factor depends on degree of cementation. The cementation factor is a central parameter in determining fluid saturations and this parameter is often assumed to equal two for carbonates but variations in the cementation factor for carbonates have been reported (Focke and Munn, 1987; Borai, 1987; Saha et al., 1993). If the cementation factor varies there is a possibility of predicting wrong fluid saturations (Borai, 1987). Only little work has been done to investigate variations in the cementation factor and further work is needed to find out what physical properties

actually control the cementation factor and explain why it varies. It would be useful to be able to predict the cementation factor based on other physical properties through a relationship between the cementation factor and physical properties that are usually known for a reservoir rock. If cementation factor depends on cementation as Archie (1942) postulated, it would be relevant to discuss the cementation factor vs. Biot's coefficient. In case a relationship exists between Biot's coefficient and the cementation factor, then the cementation factor may be predicted from Biot's coefficient. Biot's coefficient can be obtained from acoustic logging data and acoustic logging data are often available.

1.1 Scope of study

This study was divided into three parts. The first part is concerned with modeling elastic moduli and cementation of North Sea chalk. A practical measure of degree of cementation for North Sea chalk is also established. The second part of the study relates static and dynamic Young's modulus and the third part of the study investigates predictability of Archie's cementation factor.

In the first part of the study concerned with modeling elastic moduli and degree of cementation different effective medium models described in the literature were evaluated to see if they were applicable to chalk. Four different models: the Iso-Frame model, the BAM model, Berryman's self-consistent model and Dvorkin's cemented sand model were analyzed and each of the models predict two different elastic moduli based on different approaches. Each of the models also contains a parameter that is interpreted as a measure of pore space compressibility or degree of cementation. This parameter was compared to Biot's coefficient, the latter representing a measure of cementation or pore space compressibility. Based on the different models Biot's coefficient was predicted from P-wave velocity and density for water-saturated chalk. It was also discussed how consistent the different models are when two elastic moduli are modeled for dry and water-saturated chalk.

The second part of the study relates static and dynamic Young's modulus for two different kinds of North Sea chalk; Upper Cretaceous stiff cemented pure chalk and softer less cemented Lower Cretaceous marly chalk. The problem of relating static and dynamic Young's modulus was approached in two different ways for the two different kinds of chalk. For the stiff Upper Cretaceous chalk static and dynamic Young's modulus were compared directly but for the marly chalk a non-elastic deformation during static loading needs to be taken into consideration when static and dynamic Young's modulus are compared. For the Upper Cretaceous chalk main focus was on discussing the influence of the pore fluid on a possible difference between static and dynamic Young's modulus and to discuss the method for obtaining static Young's modulus. For the Lower Cretaceous chalk focus was on including non-elastic deformation when static and dynamic Young's modulus are related for softer sediments

and to develop a model to relate static and dynamic Young's modulus when significant non-elastic deformation occurs during static loading.

The third part of the study is focused on Archie's cementation factor. The aim of this study was to find out what physical properties of a reservoir rock control the cementation factor and if it was possible to predict the cementation factor from other physical properties of a reservoir rock. Prediction of Archie's cementation factor from porosity and permeability was discussed both for chalk and for published data for sandstones. Another aim of the study was to relate the cementation factor to acoustic properties through Biot's coefficient. If both Archie's cementation factor and Biot's coefficient depend on degree of cementation, then cementation factor and Biot's coefficient may be related and it may be possible to predict cementation factor from Biot's coefficient.

A central part of the study was to establish a practical measure of degree of cementation based on elastic properties. In the first part of the study on modeling elastic moduli an analysis was done on how Biot's coefficient relates to an independent measure of cementation. The independent measure of cementation was the specific surface of the chalk. Biot's coefficient was used as a measure of cementation in the part of the study about modeling of elastic moduli and in the third part of study on predicting Archie's cementation factor. The cementation aspect was to some extent included in the study on dynamic and static Young's modulus where two different sets of chalk samples the Lower Cretaceous marly chalk and the Upper Cretaceous chalk were discussed. The Upper Cretaceous chalk is more cemented where the grain contacts are stiffer than the Lower Cretaceous marly chalk and the two different kinds of chalk may behave differently due to a difference in degree of cementation.

2. Modeling elasticity and cementation of North Sea chalk

Models are made to relate elastic moduli or acoustic velocities for reservoir rocks to other rock properties such as porosity and lithology because such relations are useful in oil exploration. The theory of elasticity includes several different elastic properties P-wave modulus M, bulk modulus K, shear modulus G, Young's modulus E, Lamés parameter λ, and Poisson's ratio ν. Only two of these elastic properties are independent for an isotropic elastic material. All the different elastic parameters can be expressed as function of two other elastic properties. When elasticity of an isotropic material is modeled, two different elastic moduli need to be modeled at the same time. In case only one modulus is modeled, then elasticity of a material is not completely determined.

In this part of the study one of the main aims was to apply different kinds of effective medium models to chalk and find out if it is possible to model elasticity of chalk. Models that can predict two independent elastic moduli and contain only one free parameter were discussed. If a model include more than one free parameter, it will always be possible to model two elastic moduli just by fitting the parameters in the model. The free parameter in each of the models determines how stiff the model is for a given porosity and the free parameter is interpreted as a measure of pore space compressibility or degree of cementation. The free parameter in the models is discussed in relation to Biot's coefficient because Biot's coefficient is related to pore space compressibility. If the free parameter in a model is related to Biot's coefficient, then the free parameter is not just an arbitrary parameter but it is anchored in a physical property. This parameter may also be used to predict Biot's coefficient. It is also discussed how Biot's coefficient relates to another measure of cementation that is not an elastic property. This measure of cementation is the specific surface. The models are also used to predict Biot's coefficient based on P-wave velocity and density for water-saturated chalk and it is also discussed if the models can distinguish between sorting of chalk and degree of cementation for chalk.

Biot's coefficient is used in effective stress calculation of hydrocarbon fields and Biot's coefficient is also related to pore space compressibility. Pore space compressibility is a central parameter in reservoir simulation. If the free parameter in an effective medium model is related to Biot's coefficient then this effective medium model can be used to predict Biot's coefficient for effective stress calculations to be used in 4D seismic surveys. In case elastic properties can be used as a measure of cementation, weak zones in a reservoir may be predicted based on acoustic logging data.

2.1 Models

The problem of modeling elasticity and relationships between acoustic velocities and other parameters for a reservoir rock is an extensively studied area. Several authors

(Hertz, 1882; Voigt, 1910; Reuss, 1929; Mindlin, 1949; Brandt, 1955; Hashin and Shtrikman, 1963; Budiansky, 1965; Hill, 1965; Wu, 1966; Kuster and Toksöz, 1974; Cleary et al., 1980; Berryman, 1980; Digby, 1981; Winkler, 1983; Norris, 1985; Walton, 1987; Marion, 1990; Zimmerman, 1991; Dvorkin et al., 1994; Mukerji et al., 1995;, Dvorkin et al., 1999; Fabricius, 2003) worked on establishing effective medium models that can predict elastic moduli from different approaches. The effective medium models in the literature can be divided into bound models, wave propagation models, self-consistent models and contact theory models.

The simplest models predict the maximum upper and minimum lower bounds for elastic moduli from assumption of iso-stress or iso-strain deformation and knowledge of the volume fractions of the individual phases and the elastic moduli of the individual phases (Voigt, 1910; Reuss, 1929). Hashin and Shtrikman (1963) introduced a model that predicts a more narrow set of upper and lower bounds for elastic moduli. Nur et al. (1998) modified bound models by including the critical porosity. The bound models are not included in this study because they do not include a measure of cementation. In order to improve the models and make more precise estimates of elastic moduli in stead of bounds, it is necessary to make more specific assumptions about how the different components are geometrically arranged in a rock.

Besides the bound models other models based on bound models have been suggested by Marion (1990) and Fabricius (2003). These two models take the bound theory one step further by including information about the stiffness of the pore structure. Marion (1990) suggested a heuristic model called the bounding average method (BAM). A given rock will have elastic moduli between the upper and the lower Hashin Shtrikman bound and where it is located depends on the stiffness of the pores. The stiffness of the pores is expressed with the parameter ω given as the elastic modulus minus the lower Hashin Shtrikman bound divided by the difference between the upper and the lower Hashin Shtrikman bound

$$\omega = \frac{M - M^{-}}{M^{+} - M^{-}} \qquad (2.1)$$

where M is the measured modulus, M^{-} and M^{+} are the lower and the upper Hashin Shtrikman bound respectively. ω is assumed to be independent on pore-filling properties and only dependent on the stiffness of the pores. ω should remain constant between different pore fluids. In this study the BAM model is systematically investigated for chalk to find out if the model is consistent between dry and water-saturated chalk and if the model is consistent for two different moduli. If the model is consistent, ω should be equal for two independent elastic moduli for water-saturated and dry chalk. ω is also discussed in relation to Biot's coefficient. ω determines how stiff the model is for a given porosity therefore it is a measure of pore space compressibility or degree of cementation. But it is not interpreted as a physical property because the BAM model is a heuristic model. The BAM model is a heuristic model and it is included because it is easy to use in practical modeling.

The Iso-Frame model by Fabricius (2003) is also based on the Hashin Shtrikman bounds (Hashin and Shtrikman, 1963), but it has a more rigorous physical basis than the BAM model. The basic assumption in the Iso-Frame model is, that in chalk part of the particles is in suspension and part of the grains is in the frame. The part of the grains in the frame is characterized by the IF value and the part of the grains that are in suspension is then 1-IF. The elastic moduli of a rock are calculated from a mixture of a solid frame and a suspension of the grains that are not in the frame.

$$
\begin{aligned}
K &= K_1 + \frac{f_2}{(K_2 - K_1)^{-1} + f_1(K_1 + \frac{4}{3}G_1)^{-1}} \\
G &= G_1 + \frac{f_2}{(G_2 - G_1)^{-1} + \frac{2f_1(K_1 + 2G_1)}{5G_1(K_1 + \frac{4}{3}G_1)}}
\end{aligned}
\qquad (2.2)
$$

Where K_1 and K_2 is bulk modulus of phase 1 and 2, f_1 and f_2 is volume fraction of phase 1 and 2, G_1 and G_2 is shear modulus of phase 1 and phase 2.
In this model where part of the particles are in suspension the volume fractions f_1 and f_2 are given as

$$
\begin{aligned}
f_1 &= IF(1-\varphi) \\
f_2 &= (\varphi + (1-IF)(1-\varphi))
\end{aligned}
\qquad (2.3)
$$

Where φ is porosity. The critical porosity can also be included in the model in that case the model is a heuristic model because the critical porosity is a heuristic property. The critical porosity is the transition point between grain-supported and fluid-supported sediment (Nur et al., 1998).
For a constant IF value the part of grains in frame is the same for all porosities; going from higher porosities towards lower porosities the pore space just decreases, whereas the part of the grains in frame and suspension is constant.
The amount of grains in suspension and in frame is related to the degree of cementation because the frame is glued together by cement between the grains. The IF parameter is a measure of pore space compressibility or degree of cementation in this model. It is discussed how well the IF parameter compares to cementation as predicted by Biot's coefficient. The model is included in this study because it is the only model that is developed for chalk based on petrographical studies of chalk.

Another type of model is inclusion based models. For these models the rock is considered to be a solid frame and the pores are then put in the solid frame. One inclusion based model is developed by Kuster and Toksöz (1974). It is more complicated than the previous models because it is possible to specify the shapes of the pores and combine different pore shapes. This model only applies for low porosities because it does not account for interactions between pores. This model is not included in this study because it has too many free parameters and secondly this model does not contain a measure of cementation or pore space compressibility.

Another type of inclusion model is the self-consistent model. The self-consistent models are based on the assumption that the strain is uniform of the inclusions in an infinite background of another material. This means that the average strain of the effective medium is related to the strain of each inclusion. In the self-consistent theories each of the inclusions is an isolated inclusion in a uniform matrix. The equations that yields bulk and shear modulus are coupled equations and they must be solved numerically by iteration. A commonly used self-consistent model is developed by Berryman (1980). The model yields bulk and shear modulus from the coupled equations

$$\sum_{i=1}^{N} x_i \left(K_i - K_{sc}^*\right) P^{*i} = 0 \qquad (2.4)$$

$$\sum_{i=1}^{N} x_i \left(\mu_i - \mu_{sc}^*\right) Q^{*i} = 0 \qquad (2.5)$$

In this study the model is applied with ellipsoidal inclusions. In this case P and Q are calculated with a set of equations before the equations are solved by iteration (Berryman, 1980). i in the equations refer to the i'te material and x_i equals the volume fraction of the i'te material. P and Q are only dependent on aspect ratio of the ellipsoids (Berryman, 1980). The model is used with two different combinations of aspect ratio. The first combination is where the aspect ratio for the pores and the grains is equal and the other combination is where the aspect ratio for the pores varies and the aspect ratio for the grains is constant close to one. The aspect ratio can not equal one exactly when the model is applied with ellipsoids. The combination where the aspect ratio for the grains is constant close to one and the aspect ratio for the grains varies is not included because it is too stiff for North Sea chalk. The aspect ratio of the ellipsoidal inclusions is used as a measure of cementation or pore space compressibility and it is discussed how well the aspect ratio compares to Biot's coefficient. The self-consistent model is included in this study because it is a widely used model.

The differential effective medium theory (Cleary et al., 1980; Norris, 1985; Zimmerman, 1991) is based on adding pores to the solid. The pores are added incrementally and this process is continued until the right porosity is reached. This model was modified by Mukerji et al. (1995) by introducing the critical porosity of the rock in the model.

Elastic properties for porous rocks has also been estimated based on theories derived from mechanical analysis of spherical grains in contact (Hertz, 1882; Mindlin, 1949; Brandt, 1955; Digby, 1981; Winkler, 1983; Walton, 1987; Dvorkin et al., 1994; Dvorkin et al, 1999). The models by Hertz (1882), Mindlin (1949), Digby (1981), Winkler (1983) and Walton (1987) are not included in this study because they do not include a measure of cementation. The model by Brandt (1955) is not discussed in this study because it only models bulk modulus. In this study only models that predict two different elastic moduli are included. The model by Dvorkin et al. (1999) is not included in this study because it is derived for uncemented sediments and it is therefore not well suited for modeling chalk.

In this study the cemented sand model by Dvorkin et al. (1994) is analyzed. This model is the only grain contact model that directly quantifies the amount of cement in the rock with a certain volume of cement. Therefore it seems well suited for modeling of elasticity and degree of cementation for chalk.

The model is based on a packing of spherical grains and it can model two different cases, one where the cement is distributed along the grain surfaces and one where all the cement is located at the grain contacts. The model where all the cement is located at the grain contacts is applied because the other model is too soft for chalk. A central parameter in the model is α which is related to the porosity of the rock, φ, the porosity of the rock if the cement is removed from the rock, φ_0, and the number of grain contacts C. The parameter α is given as

$$\alpha = 2\left[\frac{\varphi_0 - \varphi}{3C(1-\varphi_0)}\right]^{0.25} \qquad (2.6)$$

The modeled bulk modulus, K_{eff}, and shear modulus, G_{eff}, are calculated with these equations (Mavko et al. 1998):

$$K_{eff} = \frac{1}{6}C(1-\varphi_0)M_c S_n \qquad (2.7)$$

$$G_{eff} = \frac{3}{5}K_{eff} + \frac{3}{20}C(1-\varphi_0)G_c S_t \qquad (2.8)$$

Where M_c is the P-wave modulus of the cement between the grains, G_c is the shear modulus of the cement, and S_n and S_t are proportional to the normal and shear stiffness of two cemented grains. Calculation of S_n and S_t is based on a numerical solution by Dvorkin et al. (1994). S_n and S_t are given as functions of the parameter α (Mavko et al., 1998):

$$S_n = A_n\alpha^2 + B_n\alpha + C_n \qquad (2.9)$$

$$S_t = A_t\alpha^2 + B_t\alpha + C_t \qquad (2.10)$$

For calculation of A, B and C see Mavko et al. (1998).
In this model φ_0-φ is then the volume of cement in the model because φ_0 equals the porosity if all the cement is removed. C is the number of contacts and this number is defined by porosity which is known in this study for all rock samples modeled. This means that the volume of cement, φ_0-φ, is the only free parameter in this model.

2.2 Pore space compressibility and degree of cementation

Pore space compressibility in a sediment depends strongly on cementation at grain contacts that glues the grains together. Cementation of North Sea chalk occurs

when calcite is precipitated around grain contacts and on the surface of the grains. Cement around grain contacts will increase the stiffness of the rock and the more cement at the grain contact the stiffer the rock will be.

One property that gives an indication of pore space compressibility is the Biot coefficient. Biot's coefficient is calculated from dynamic elastic moduli with the equation

$$\beta = 1 - K_{dry}/K_0 \quad (2.11)$$

see e.g. Mavko et al. (1998) where K_{dry} is the dynamic dry bulk modulus and K_0 is the dynamic bulk modulus of the matrix mineral. The upper limit for Biot's coefficient is 1 and it corresponds to a rock without cement at the grain contacts because K_{dry} has a finite small value close to zero. When Biot's coefficient equals one the rock acts as a suspension and the stiffness of the rock is described with the Reuss bound (Reuss, 1923). The lower limit for Biot's coefficient equals the porosity of the rock. Biot's coefficient equal to porosity of a rock corresponds to the stiffest possible arrangement of the grains, a Voigt bound (Voigt, 1910), where cementation in the grain contacts cannot make the rock stiffer (Fjaer et al., 1992). Biot's coefficient only equals zero when the porosity equals zero corresponding to $K_{dry}=K_0$. This means that Biot's coefficient can be used to evaluate where a given rock is located between the maximum degree of cementation at the grain contacts (Voigt bound) or minimum degree of cementation at the grain contacts. Biot's coefficient is directly related to pore space compressibility through the relationship

$$\beta = \frac{\varphi K_{dry}}{K_{\varphi}} \quad (2.12)$$

see e.g. Mavko et al. (1998), where β is Biot's coefficient, φ is porosity, K_{dry} is dry bulk modulus and K_φ is pore space compressibility. Biot's coefficient was used as a measure of cementation for water-saturated chalk from the North Sea by Gommesen et al. (2007).

Biot's coefficient can also be used to calculate effective stress in a rock. A general effective stress law was introduced by Brandt (1955) and later by Biot and Willis (1957) where the pore pressure in effective stress calculations is multiplied by a factor called the effective stress coefficient. Biot and Willis (1957) showed that the effective stress coefficient is less than one. Nur and Byerlee (1971) suggested a general effective stress equation as

$$\sigma' = \sigma - nP_p \quad (2.13)$$

where σ is confining stress, σ' is effective stress and n equals $n = 1 - K_{dry}/K_0$. This expression for n was analytically derived and it was also suggested by Gertsma (1957). Under ideal elastic conditions n equals Biot's coefficient, β.

2.3 Biot's coefficient as a measure of degree of cementation

Biot's coefficient is in this study used as a measure of pore space compressibility and degree of cementation. If Biot's coefficient is a good measure of

pore space compressibility and degree of cementation it should be in agreement with another measure of cementation, the specific surface. Biot's coefficient should also only depend little on mineralogy and texture.

When cementation occurs, calcite is precipitated on the grain surfaces and in the grain contacts. This process will decrease the specific surface with respect to grain volume for chalk because cementation tends to smooth irregularities and because the grain volume will increase when calcite is precipitated on the grain surface. The specific surface with respect to the pore volume will increase because the pore volume decreases at a greater rate than the grain pore interface (Borre and Fabricius, 1998). In order to study the influence of cementation on specific surface, the measured specific surface is normalized with respect to pore volume and pore space. Biot's coefficient is close to one for samples with a low degree of cementation and decreases for a higher degree of cementation because the cementation strengthens the grain contacts. When Biot's coefficient is compared to the specific surface, the texture and mineralogical composition is also taken into consideration (Figure 2.1a-b). As expected, Biot's coefficient of the calcite rich samples (more than 95 % calcite) decreases with decreasing specific surface relative to grain volume and decreases with increasing specific surface with respect to the pores. The samples with a higher content of quartz and clay have a relatively high specific surface for a given Biot's coefficient. All samples contain a different volume of quartz and clay (Manuscript 1, Table 2), but in accordance with Røgen and Fabricius (2002) there is a small variation in the amount of clay in the samples (Manuscript 1, Table 2) and the clay is dominantly smectite. I therefore expect that clay has a more or less constant influence on the specific surface of the samples. This indicates that the content of quartz has a significant influence on the specific surface of the chalk. We find that the specific surface is higher for the samples with a high content of quartz. This could be due to effects from a small sized quartz crystal, but it could also be an influence from quartz on the specific surface of the calcite. The texture of the sample does not have an influence on the specific surface of the samples (Figure 2.1a-b). This means that a relationship between cementation and Biot's coefficient can be seen from the specific surface of calcite rich samples, whereas for quartz rich samples it is difficult to detect the relationship between Biot's coefficient and the specific surface.

Biot's coefficient decreases with decreasing porosity (Figure 2.1c). The influence of texture is on porosity (Figure 2.1c). The wackestones and the mudstones follow the same trend line but mudstones tend to be more porous and have a higher Biot's coefficient than wackestones. There is only one packstone included in Figure 2.1c. This packstone is located above the main trend line, which means that it probably is less cemented than the samples in the main trend line (Figure 2.1c).

From the discussion on Biot's coefficient, it appears that Biot's coefficient is related to the specific surface of the samples. The specific surface is related to degree of cementation. So the analysis confirms that Biot's coefficient is a measure of cementation in the studied samples. For a given porosity Biot's coefficient is only little influenced by the texture and mineralogical composition.

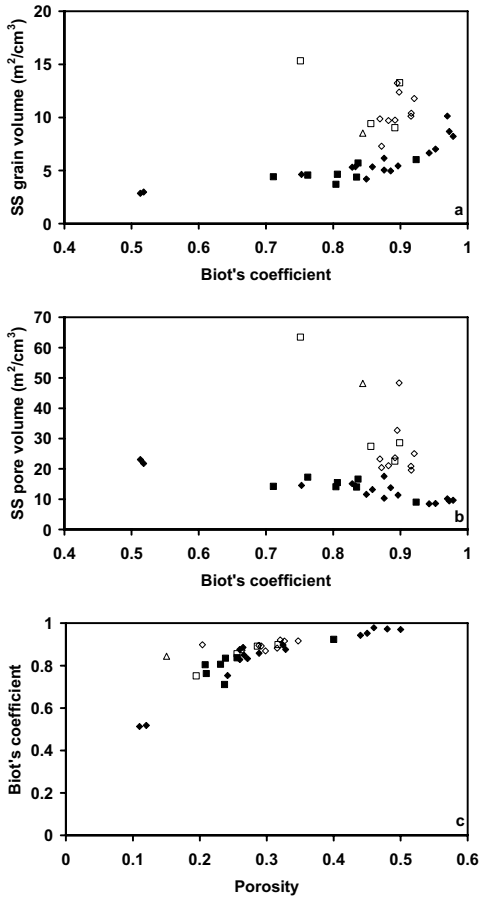

Figure 2.1a-c. a,b: Specific surface as measured by BET vs. Biot's coefficient of the chalk samples. a: The specific surface is normalized to the grain volume. b: The specific surface is normalized to the porosity. c: Biot coefficient vs. porosity. In all plots filled signature represents a carbonate content higher than 95% and hollow signature represents a carbonate content lower than 95%. In all plots diamond is mudstone texture, square is wackestone texture and triangle is packstone texture.

2.4 Consistency of models

One of the aims of in this part of the study is to find out how consistent the different models are when two elastic moduli are modeled at the same time for water-saturated and dry chalk. If a model is consistent the free parameter in the model should be the same when different elastic moduli are modeled for dry and water-saturated chalk. For each of the models the free parameter needed to model P-wave modulus and shear modulus for dry and water-saturated chalk is obtained and this parameter is used to discuss consistency of the models. For the cemented sand model it is not possible to obtain the free parameter for two different moduli due to the nature of the model. In this case modeled elastic moduli are discussed versus elastic moduli for the samples. In all the models elastic properties of the solid phase are those of clean calcite. The insoluble residue is not included in the modeling because the mineralogical composition does not have a great influence on results in modeling chalk unless the content of insoluble residue is very high (Fabricius et al., 2007).

For the Iso-Frame model, the BAM model and Berryman's self-consistent model consistency is analyzed the same way for the different models. The free parameter needed to model two different elastic moduli is plotted versus each other. In this case two different groups of paired data are compared for a number of samples and the normal way to compare such populations would be to apply a paired t-test. A paired t-

test determines whether two paired obtained values differ from each other significantly. It is assumed in the paired t-test that the differences between the paired data are independent and normally distributed. The paired t-test is normally a powerful statistical tool but it is not applicable here because the data compared are not normally distributed. The chalk samples where chosen to be as different in porosity and mineralogy as possible and for this reason the data are not normally distributed and the paired t-test can not be used. An alternative statistical test to compare two paired groups of data is the Wilcoxon matched pairs signed ranks test, this test is a non-parametric test, and it is not dependent on a normal distribution of data. This test assumes that there is information in the magnitude and sign of the differences between the two groups of data. If this test is carried out to compare two data sets that seem almost equal, the test indicates that the model is not even close to being consistent. Instead of applying a rigorous statistical test the mean of the difference between the free parameter for the two moduli and the standard deviation of the difference between the free parameter for the two moduli are discussed. These two simple parameters show in a simple way how close the free parameter for the two different moduli is to each other but they do not give a very strict statistical measure of how consistent the model is.

2.4.1 Iso-Frame model

The Iso-Frame model is analyzed as a physical model without a critical porosity. For the Iso-Frame model the IF value is the only free parameter because the porosity is fixed for the samples. First consistency between P-wave modulus and shear modulus is analyzed for dry and water-saturated chalk (Figure 2.2a). For both dry and water-saturated chalk IF for shear modulus is slightly larger than IF values for P-wave modulus. The error between the IF value for shear modulus and for P-wave modulus is almost constant. The IF value for P-wave modulus for dry chalk compared to the IF value for P-wave modulus for water-saturated chalk yields the best agreement between IF values (Figure 2.2b); the mean of the differences in the IF value is as low as 0.017 and the standard deviation for the differences is 0.02. IF values for dry shear modulus is larger than IF values for water-saturated shear modulus. IF values are in all cases close to each other and form well defined straight lines with high R^2. The model is least consistent between dry and water-saturated shear modulus. The Iso-Frame model is developed for chalk based on observations of chalk on a microscopical scale. The differences in the IF value between the different moduli can be due to different reasons. The model is based on the Hashin Shtrikman model. If the Hashin Shtrikman model is not consistent between two different moduli then the Iso-Frame model will not be consistent between two different moduli. If the modulus in the Hashin Shtrikman model does not vary with porosity the same way as the measured modulus does for two different moduli, then the model will not be consistent between two different moduli. That the model is not consistent between dry and water-saturated shear modulus can perhaps be explained from the physics of chalk. When North Sea chalk is saturated with water the chalk is weakened by the water (Risnes and Flaageng, 1999). This could have an influence on the modeled IF value since this water weakening effect is not included in the model. The P-wave modulus could be less sensitive to this water weakening effect since the model is more

consistent from dry to water-saturated P-wave modulus. It does not make the model more consistent if a critical porosity below 100 % is included in the model (Manuscript 1).

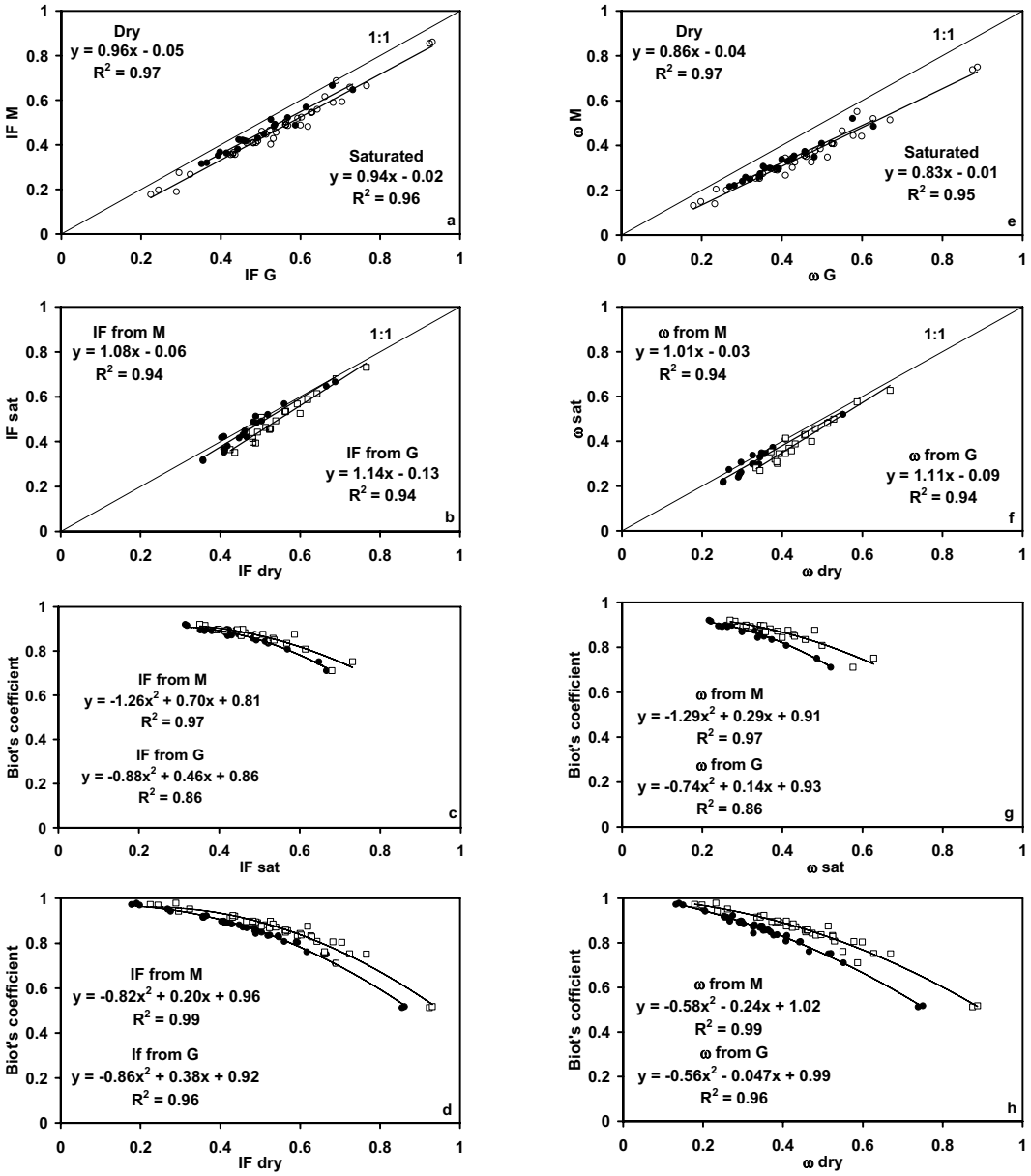

Figure 2.2a-h. a-d: IF from the Iso-Frame model for P-wave modulus (M) and shear modulus (G). a: IF needed to model M vs. IF needed to model G. Filled dots are water-saturated data and hollow dots are dry data. b: IF needed to model water-saturated data vs. IF needed to model dry data. Filled dots are P-wave modulus and open square is shear modulus. c,d; Biot coefficient vs. IF needed to model water-saturated and dry M and G. P-wave modulus is dots and shear modulus is squares. e-h: is the same combination of plots with the ω-value for the BAM model.

2.4.2 BAM model

Consistency of the BAM model is analyzed based on Figure 2.2e-f. If the BAM model is consistent, the ω parameter should be the same for both P-wave modulus and shear modulus for dry and water-saturated chalk. The porosity for the samples is fixed and so there is only one free parameter in the model, the ω value. For both saturated and dry chalk ω for shear modulus is larger than ω for P-wave modulus and the difference increases with increasing ω value (Figure 2.2e). The same type of analysis is done to find out if the model is consistent from dry to saturated chalk (Figure 2.2f). For the P-wave modulus the model is consistent and the mean of the differences between the ω value for dry and water-saturated chalk is as low as 0.024 and the standard deviation is as low as 0.024. ω for shear modulus for dry chalk is always larger than ω for water-saturated chalk and the error between ω for dry and water-saturated chalk increases with decreasing ω. Similarly Røgen et al. (2004) found that v_p for saturated chalk can be predicted from v_p for dry chalk consistently by using the BAM model. But even though ω is not completely equal between two different moduli in three cases the model is reasonable. ω values in the cases where the model is not completely consistent are still close to each other and ω values always form well defined straight lines with high R^2. The reasons why this model is not completely consistent are the same as the reasons why the Iso-Frame model is not completely consistent.

2.4.3 Berryman's self-consistent model

The self-consistent model by Berryman (1980) can be used with several different combinations of aspect ratio for the pores and the grains. In this study models with only one free parameter are discussed, so in this study Berryman's self-consistent model is restricted to one free parameter. The first case to analyze is where the aspect ratio for the pores and the solids are equal and both vary, the other case is where the aspect ratio for the solid part is kept constant close to one and the aspect ratio of the pores varies. When the aspect ratio of the solids is close to one, the grains are almost spherical. The aspect ratio can not equal one exactly when the pores and grains are described as ellipsoids.

For the first case where the aspect ratio is equal for pores and grains the consistency between P-wave modulus and shear modulus is analyzed based on Figure 2.3a. For both the dry and water-saturated case the model is consistent and aspect ratio is distributed along the 1:1 line. In the dry case the mean of the difference between the aspect ratio is 0.06 and the standard deviation is 0.29. The relatively high mean and standard deviation is because of the samples from the Valhall field have high aspect ratios and the differences between them are larger than for the small aspect ratios. The self-consistent model does a less good job in modeling the Valhall samples with porosities above 40%. For the water-saturated case the Valhall samples are not included in the analysis because data for water-saturated chalk does not exist for the samples from the Valhall field. The mean of the differences in the aspect ratio for P-wave and shear modulus is for the water-saturated chalk 0.0004 and the standard deviation is 0.013. The model is consistent between P-wave and shear modulus for one fluid. The

same analysis is done when the model is compared from water-saturated to dry chalk and in this case it is clear that the model is not consistent (Figure 2.3b). The aspect ratio for the dry chalk is significantly larger than the aspect ratio for the water-saturated chalk for both P-wave modulus and shear modulus.

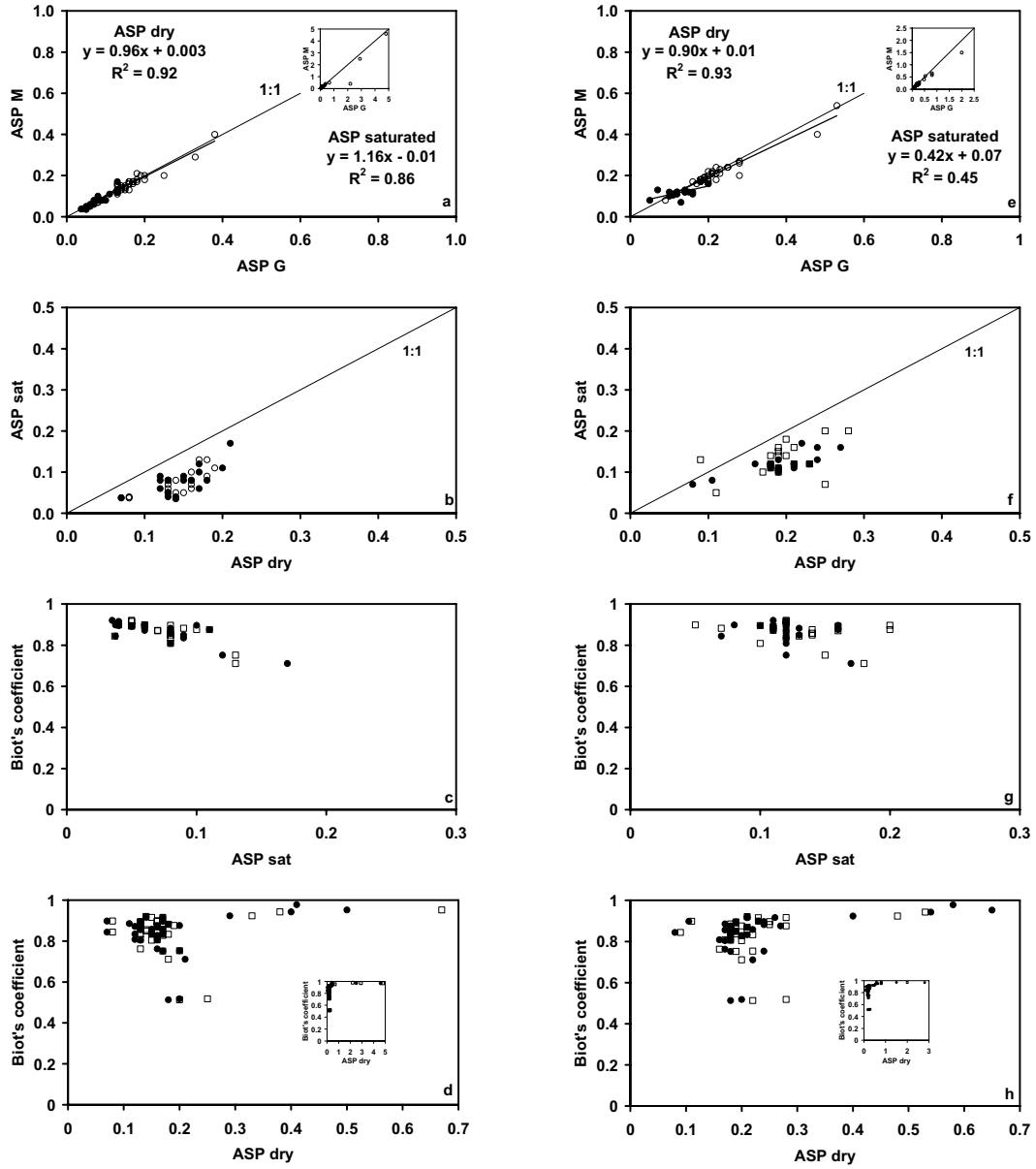

Figure 2.3a-h. a-d: is aspect ratio from the self consistent model by Berryman (1980) for P-wave modulus (M) and shear modulus (G) where aspect ratio for pores and grains are equal. a: Aspect ratio needed to model M vs. aspect ratio needed to model G. Filled dots are water-saturated data and hollow dots are dry data. b: aspect ratio needed to model water-saturated data vs. aspect ratio needed to model dry data. Filled dots are P-wave modulus and hollow squares are shear modulus. c,d: Biot's coefficient vs. aspect ratio needed to model water- saturated and dry M and G. P-wave modulus is dots and squares are shear modulus. e-h: The same combination of plots with the aspect ratio for the pores when the aspect ratio for the grains is kept constant at 0.99. For figure a, d, e and h a smaller figure with other axis is placed inside the figure in order to show all data.

The second case for the self-consistent model by Berryman (1980) is where the aspect ratio for the grains is kept constant close to one and the aspect ratio for the pores varies (Figure 2.3e-f). In the dry case the aspect ratio for the P-wave modulus and shear modulus is similar to each other and close to a 1:1 relationship (Figure 2.3e); the mean of the differences between the aspect ratio is 0.03 and the standard deviation is 0.09. In this case the model also has a problem with the Valhall samples, these samples have high aspect ratios and they are not as consistent between two different moduli as the samples with low aspect ratios. In the water-saturated case the aspect ratio is also distributed around the 1:1 line and consistent. For the low aspect ratios a few samples are located above and below the 1:1 line which gives the regression line a low slope (Figure 2.3e). But the mean of the differences between the aspect ratio is low 0.01 and the standard deviation is 0.03. The model is not consistent from water-saturated to dry chalk; the aspect ratio is much larger for the dry samples than for the water-saturated samples (Figure 2.3f).

In both cases the model is consistent between two different moduli with the same pore fluid. The set of equations yielding bulk modulus and shear modulus are solved simultaneously and it therefore provides consistent values of the aspect ratio. But it is clearly not the same aspect ratio in the dry and water-saturated case; the dry and the water-saturated chalk solution does not seem to be related. The reason for this difference may be due to water-weakening as described for the Iso-Frame model, it may also be due to a general problem with the model.

2.4.4 The cemented sand model

The cemented sand model is the only model that directly quantifies the degree of cementation with a certain volume of cement. The model only models dry chalk and it is only able to model bulk modulus up to 15 GPa and based on bulk modulus shear modulus is modeled. The model is only able to model shear modulus for the softest samples. For the stiffer samples the model systematically over-predicts the shear modulus (Figure 2.4a-b).

As the analysis of the model shows the cemented sand model is not consistent for chalk between bulk and shear modulus, therefore the model is not applicable to chalk. In the derivation of the model it is assumed that the rock consists of a random packing of spherical grains with a critical porosity around 36% and with only small amounts of cement in the grain contacts. This physical approach does not describe North Sea chalk and it may be a reason why this model does a less good job in modeling elastic moduli for chalk. The model is derived for sandstones and based on Dvorkin et al. (1994), it is not clear how the equations for calculating bulk and shear modulus was obtained. Since the model is derived for sand, some of the parameters in the model may be dependent on properties for quartz. Bulk modulus and shear modulus are different for quartz and calcite. If the model is dependent on quartz properties it could be the reason why it over predicts shear modulus. A numerical method was therefore applied to solve the equations in Dvorkin et al. (1994) to find out if it would provide a more consistent solution. But the numerical solution made in this study did not make the model more consistent for chalk. Another problem about the cemented sand model by Dvorkin et al.

(1994) is that it models bulk and shear modulus with a constant ratio between bulk modulus and shear modulus independent on porosity. For chalk the ratio between bulk modulus and shear modulus depends on porosity.

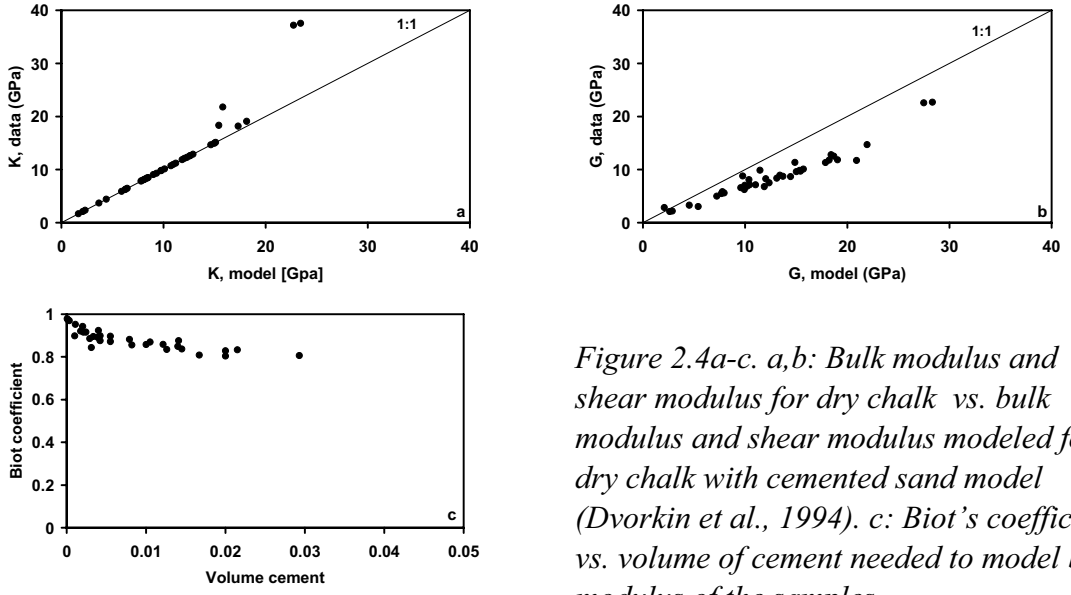

Figure 2.4a-c. a,b: Bulk modulus and shear modulus for dry chalk vs. bulk modulus and shear modulus modeled for dry chalk with cemented sand model (Dvorkin et al., 1994). c: Biot's coefficient vs. volume of cement needed to model bulk modulus of the samples.

2.5 Input parameters in the models

The input parameters in the models are also a source of inconsistencies for the models used in this study. The different input parameters are not equally well known and they do not contribute to inconsistencies equally. Porosity is well known for the samples in this study, it can be measured with a little uncertainty. The porosity should only have a limited influence on inconsistencies for the different models.

A parameter that has a large influence on elastic moduli predictions is the elastic moduli for zero porosity. All the models in this study assume that elastic modulus for a crystal of calcite can be used as the endpoint for zero porosity. This is probably the weakest point in the models. The end point in the model should in stead be a value that characterizes the stiffness of a packing of grains with infinitely low porosity where the moduli of the grains in contact is reflected and not the solid crystals elastic moduli. There is a large discontinuity going from a rock with a low porosity that consists of individual grains in contact to a solid crystal.

Elastic properties of the water used to saturate the rocks are another source of inconsistency. In the pore space small air bubbles may exist and air bubbles can influence dramatically on the elastic properties of the water dependent on how the air bubbles are distributed in the water. If air is mixed with water according to a Reuss bound, even small amounts of air can have a significant influence on the elastic properties of the elastic modulus (Kieffer, 1977). In this study on modeling elastic properties, the modulus of the water is the modulus of the water at room temperature where the air that may exist in the pores is not taken into consideration.

2.6 The free parameter vs. Biot's coefficient

The other main aim in the study is to find out if the free parameter in the different models that describe degree of cementation or pore space compressibility is consistent with the Biot coefficient.

2.6.1 Iso-Frame and BAM model

For the Iso-Frame model the free parameter, IF, is related to degree of cementation and pore space compressibility for chalk. For lower values of IF chalk must have a low degree of cementation and for higher values of IF chalk must have a higher degree of cementation. IF is compared to Biot's coefficient for both P-wave modulus and shear modulus for dry and water-saturated chalk. The expected relationship between IF and Biot's coefficient is negative but not necessarily linear for the entire span of IF and Biot's coefficient. The IF value is compared to Biot's coefficient (Figure 2.2c-d). In all four different cases where IF has been obtained for P-wave and shear modulus for dry and water-saturated chalk Biot's coefficient decreases as IF increases as expected. The relationship between Biot's coefficient and IF can not be approximated with a straight line. Here the relationship is approximated with a polynomial of the second degree; the polynomial approximation is in this case a good approximation with high R^2 values. The relationship between Biot's coefficient and IF can not be approximated with the same polynomial in all cases because the model is not 100% consistent between all moduli for dry and water-saturated chalk; and because there are more dry data than water-saturated data and because the dry data set includes samples with higher Biot's coefficients and lower IF values. The dry samples cover a larger span of Biot's coefficient versus IF value than the water-saturated samples. The relationship between Biot's coefficient and the IF value outside the interval covered by the data is discussed based on the dry data. No samples has a Biot's coefficient equal to 1, the highest is around 0.97. IF must equal 0 for Biot's coefficient equal to 1. So the relationship between IF and Biot's coefficient must become very flat above Biot's coefficient equal to 0.97 and go towards IF equal to 0 for Biot's coefficient equal to 1. The highest value for IF for the dry samples is around 0.9 and Biot's coefficient around 0.5. For higher values of IF the relationship between Biot's coefficient should be more steep than the trend line shown (Figure 2.2d). The lower value is not simply zero because Biot's coefficient only equals zero when the porosity is zero. The IF value seems to be related to pore space compressibility and cementation. For the BAM model similar relationships between the free parameter, ω, and Biot's coefficient is obtained (Figure 2.2g-h).

2.6.2 Berryman's self-consistent model

For the self-consistent model the aspect ratio is discussed in relation to Biot's coefficient for the two different combinations of aspect ratios. The aspect ratio is the measure of pore space compressibility or degree of cementation in the Berryman self-consistent model because it determines how stiff the rock is for a given porosity. The aspect ratio in the self-consistent model is related to Biot's coefficient for water-

saturated chalk where the aspect ratio for the pores and the grains are equal (Figure 2.3a), and we find that the aspect ratio increases with decreasing Biot's coefficient. If the aspect ratio increases then the stiffness of the rock should increase and consequently Biot's coefficient should decrease. The aspect ratio is not related to Biot's coefficient for dry chalk when the aspect ratio for pores and grains is equal (Figure 2.3b). For the combination of the self-consistent model where aspect ratio for the grains is constant close to one and the aspect ratio of the pores varies, the aspect ratio is not related to Biot's coefficient. In this case the aspect ratio may be a too abstract parameter to relate to Biot's coefficient or pore space compressibility.

2.6.3 The cemented sand model

The cemented sand model by Dvorkin et al. (1994) is the only model that directly includes the cementation as a volume of cement. The volume of the pore space occupied by the cement is clearly related to the Biot coefficient and pore space compressibility (Figure 2.4c). High values of Biot's coefficient corresponds to a low degree of cementation, the volume of cement is very low. When Biot's coefficient decreases the degree of cementation increases and the volume of cement in the model increases. In the discussion of volume cement versus Biot's coefficient only samples where the bulk modulus can be modeled is included. For the cemented sand model the volume of cement is therefore in agreement with physical properties related the pore space compressibility and degree of cementation.

2.7 Sorting and cementation

It was also analyzed if the effective medium models are able to distinguish between sorting and cementation. Sorting and cementation can both reduce the porosity but they do not increase the elastic properties equally. A decrease in degree of sorting will reduce the porosity but only increase the stiffness slightly. An increase in degree of cementation may reduce the porosity but the stiffness of the chalk will increase significantly. This analysis is done based on Figure 2.5a-e. This figure shows Biot's coefficient vs. porosity for different values of the free parameter for the different models. The dry bulk modulus is calculated as a function of porosity for different values of the free parameter in the different models and Biot's coefficient is then calculated as a function of porosity with the equation $\beta = 1 - K_{dry} / K_0$.

If a model is able to distinguish between sorting and cementation the type curves for Biot's coefficient vs. porosity should be clearly separated from each other. The type curves for Biot's coefficient vs. porosity starts at Biot's coefficient equal to one for 100% porosity and decreases towards zero for decreasing porosity for the BAM model and the Iso-Frame model (Figure 2.5a-b). The curves are clearly distinct for porosities below 60%. The models are clearly able to differentiate different degrees of cementation. For very high porosities the curves are close to each other and they have the same value for 100% porosity. For the cemented sand model (Figure 2.5e) the trend curves behave the same way as for BAM and Iso-Frame model. The trend curves are

clearly separated from each other. The model only goes up to 70% because this is the largest porosity where the number of contacts between spherical grains is known (Mavko et al. 1998). The number of contacts is included in calculation of the bulk modulus.
Figure 2.5c-d shows Biot coefficient vs. porosity for Berryman self-consistent model, Figure 2.5c represents the case where aspect ratio is equal for pores and solids and Figure 2.5d represents the case where aspect ratio is constant close to one for the solids. For the lowest aspect ratios 0.01, 0.1, 0.2 and 0.3 there is a clear distance between the different trend curves but for higher aspect ratios the trend curves are almost the same all of them. The self-consistent model does not distinguish between sorting and cementation as well as the other models does.

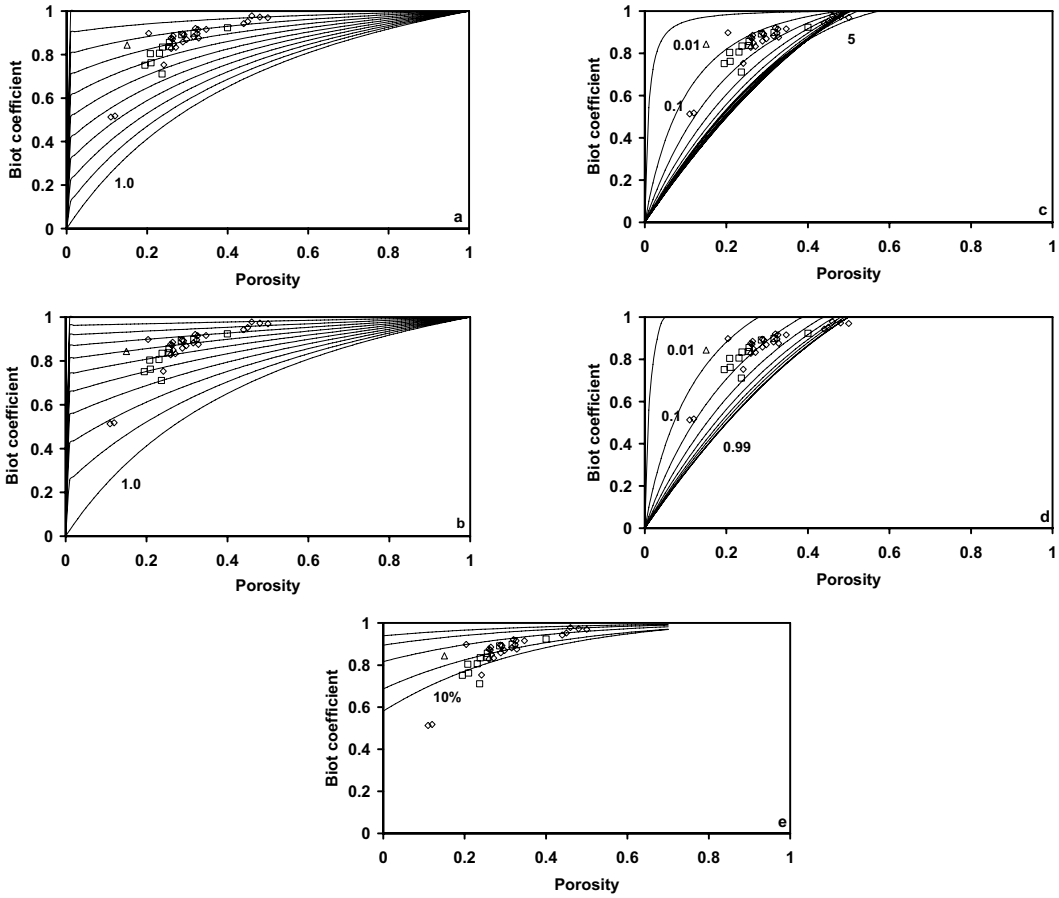

Figure 2.5 a-e. Type curves for Biot's coefficient calculated from dry bulk modulus vs. porosity for the different models. a: Biot's coefficient from the BAM model. The distance between each type curve is 0.1. b: Type curves for Biot's coefficient based on the Iso-frame model. The distance between each type curve is 0.1. c: Type curves for Berryman model where aspect ratio for pores and grains is equal. The first type curve is for aspect ratio 0.01 and the last one is for aspect ratio 5. d: Type curves for Berryman's model where aspect ratio is constant 0.99 for the grains. The first type curve is for aspect ratio 0.01 and the last one for 0.99. e: Biot's coefficient for the cemented sand model by Dvorkin et al. (1994). The lower curve is for 10% volume cement and for the following type curves the volume of cement decreases by one order of magnitude. The texture of the samples is indicated with the signature, diamond is mudstone, square is wackestone and triangle is packstone.

2.8 Estimating Biot's coefficient from P-wave velocity and density for water-saturated chalk

To find out how well Biot's coefficient can be predicted if only P-wave velocity and density is available are interesting because usually when elastic properties are evaluated in situ based on logging data the porosity, density and acoustic P-wave velocity are known for saturated rock. For each of the models Biot's coefficient is predicted based

on the saturated P-wave modulus. The prediction is not done for the cemented sand model because it does not model saturated rock. The first step is to find the free parameter in each of the models for the saturated P-wave modulus and use this parameter to predict the dry bulk modulus by assuming that the model is consistent. Based on the predicted dry bulk modulus Biot's coefficient is calculated and compared to Biot's coefficient calculated based on the measured dry velocity data. Biot's coefficient based on P-wave and S-wave velocities for dry chalk versus the predicted Biot's coefficient is shown Figure 2.6a-d. None of the models are able to predict Biot's coefficient from the saturated P-wave modulus consistently for all the samples because the models are not completely consistent from water-saturated to dry chalk. The BAM model does a good job in predicting Biot's coefficient for the highest values of Biot's coefficient where the error is around 1% to 2%. For a Biot's coefficient from 0.7 to 0.85 the error is in the interval 3 % to 8 % (Figure 2.6a). The Iso-Frame model does similarly to the BAM model a good job in prediction the Biot's coefficient for high values of Biot's coefficient where the error is 1% to 2% and for Biot's coefficient in the interval from 0.7 to 0.85 the error is 3 % to 7 % (Figure 2.6b). For the self-consistent model by Berryman (1980) where the aspect ratio for the grains and the pores is equal the model predicts Biot's coefficient with a more or less constant error around 5 % to 7 %, the error is highest for the highest Biot's coefficient (Figure 2.6c). For the self-consistent model where aspect ratio for the grains is kept constant the error between the predicted Biot's coefficient and the Biot's coefficient based on the measured dry velocity is in the interval 4 % to 15 % and the error is not systematic (Figure 2.6d).

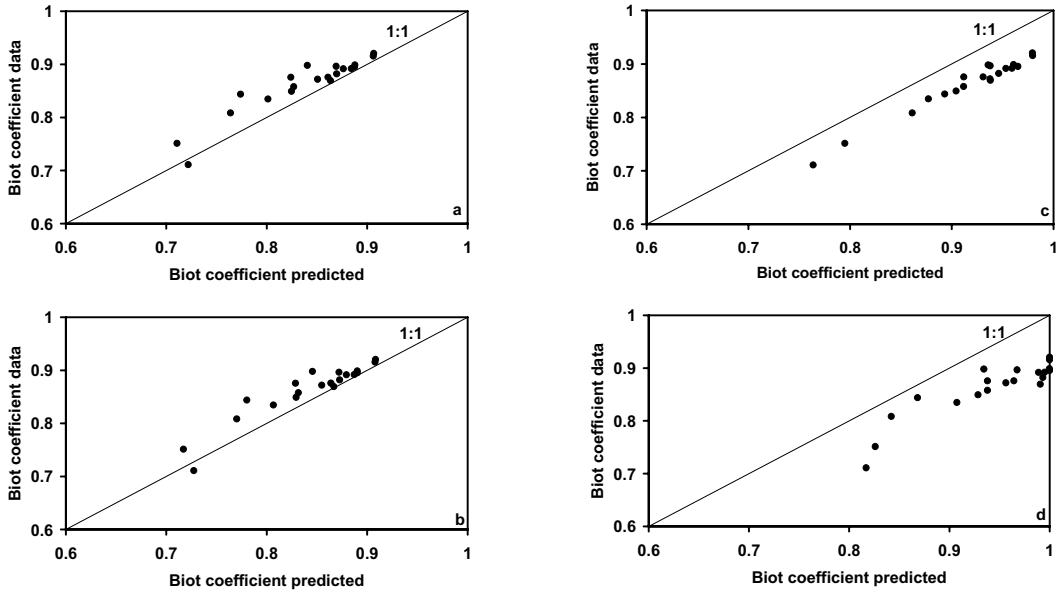

Figure 2.6a-d. Biot coefficient calculated from measured acoustic velocities and density on dry rock vs. predicted Biot's coefficient from the different models based onP-wave velocity and density for water-saturated chalk. a: Biot's coefficient predicted based on the BAM model. b: Biot's coefficient predicted based on the Iso-Frame model. c: Biot's coefficient predicted based on the self-consistent model where the aspect ratio for the pores and the grains is equal. d: Biot's coefficient predicted based on the self-consistent model where the aspect ratio for the grains is kept constant at 0.99.

3. Static and dynamic Young's modulus

Elastic moduli of a reservoir rock control in situ deformation of a hydrocarbon reservoir during production of hydrocarbon due to changes in effective stress. Elastic moduli can be obtained from acoustic measurements often called dynamic moduli and from rock mechanics loading experiments often called static moduli. Frequency and strain amplitude are obvious differences between the two different methods for obtaining elastic moduli. Acoustic velocities and dynamic moduli for a reservoir rock are often obtained from log data with a frequency in the kilo Hertz interval and static modulus is obtained at a frequency close to zero in rock mechanics experiments. The stain amplitude is several orders of magnitude higher in the rock mechanics experiment than for the acoustic measurements.

Two different studies were done to discuss static versus dynamic Young's modulus for chalk. The first study was done on Lower Cretaceous marly chalk from the Valdemar oilfield in the North Sea. In this part of the study the chalk samples experience significant non-elastic deformation during rock mechanical loading. In this part of the study the aim was to include non-elastic deformation when static and dynamic moduli are discussed for softer rocks and to make a model that relates static and dynamic modulus when significant non-elastic deformation occurs during rock mechanical loading. The other study was done for Upper Cretaceous chalk. For the Upper Cretaceous chalk samples, static Young's modulus was obtained where the samples deformed close to linear elastic. The main aim in this study was to discuss the influence of pore fluid on a possible difference between dynamic and static Young's modulus and to discuss different methods for obtaining static Young's modulus.

Static Young's modulus is obtained from uniaxial compression test where a cylindrical rock sample is exposed to force from the end surfaces in a triaxial cell and confining stress on the sample is kept constant. Stress and axial strain is obtained during loading and the slope of the stress strain curve is the Young's modulus.

$$E = \frac{d\sigma}{d\varepsilon} \quad (3.1)$$

The dynamic Young's modulus is dependent on density of the rock and P- wave and Shear wave velocities, v_p and v_s.

$$E = \rho v_s^2(4v_p^2 - 3v_s^2)/(v_p^2 - v_s^2) \quad (3.2)$$

3.1 Comparing static and dynamic moduli

Several authors worked with comparing static and dynamic modulus (Simmons and Brace, 1965; Cheng and Johnson, 1981; Montmayeur and Graves, 1985; van Heerden, 1987; Jizba et al., 1990; Tutuncu and Sharma, 1992; Tutuncu et al., 1994;

Yale and Jamieson 1994; Yale et al. 1995; Plona and Cook, 1995; Tutuncu et al., 1998; Henriksen et al., 1999; Fjær, 1999; Wang, 2000; Gommesen and Fabricius, 2001; Al-Tahini et al., 2004).

Simmons and Brace (1965) measured compressibility (inverse of bulk modulus) for different rock types. They found a good agreement between static and dynamic properties for high stresses but not for low stresses. They suggested that the disagreement between static and dynamic modulus is caused by fractures in the rock.

Cheng and Johnson (1981) measured static and dynamic bulk modulus for sandstone, limestone, granite and oil shale samples. They measured static modulus based on strain gauges and acoustic velocities were obtained with pulse transmission method with a frequency of 1MHz. They obtained a ratio around 2 between dynamic and static bulk modulus for low stresses and the ratio decreased to around 1 when the stress increased to 200 MPa. Cheng and Johnson (1981) suggested that non-linear elastic deformation during mechanical loading can cause a difference between static and dynamic modulus because non-elastic deformation does not occur in dynamic measurements. They also suggested that micro cracks in rocks can cause a difference between static and dynamic modulus because micro cracks will influence differently on static and dynamic modulus. The static measurement is more influenced by a crack in a rock because it makes the rock softer when the rock is deformed with a large strain amplitude. They base the conclusions on the fact that the rocks in their study act stiffer under high confining stress. The fractures should be closed at high confining stress and they should be open at low confining stress.

Montmayeur and Graves (1985) studied saturated consolidated and unconsolidated sandstones. They measured Young's modulus for drained rock based on LVDT (Linear Voltage Displacement Transducer) and the acoustic measurements were done with pulse transmission method with a frequency around 800 kHz for P-wave velocity and 500 kHz for S-wave velocity. Montmayeur and Graves (1985) did not obtain any clear relationship between static and dynamic Young's modulus.

Van Herden (1987) measured static and dynamic Young's modulus for dry sandstones and hard rocks. The static Young's modulus was obtained with strain gauges and dynamic Young's modulus was obtained with pulse transmission method and static and dynamic Young's modulus was obtained at the same stress level. The aim of the study was to establish a relationship between static and dynamic modulus for the different rock types. This relationship is given as $E_s = aE_d^b$ where a and b are coefficients specific for the different rock types used in the study. The ratio between dynamic and static Young's modulus varies in the interval 1-3.

Jizba et al. (1990) worked with dry sandstones with porosity in the interval 0.2% to 12% and they obtained dynamic bulk modulus from pulse transmission method with a frequency of 1MHz and static bulk modulus is obtained from strain gauges. Jizba et al. (1990) showed that the ratio between dynamic and static bulk moduli depends on the stress in the interval 5-125 MPa and the content of clay in the samples. The ratio between dynamic and static bulk modulus for the sandstones is 1.1-1.6.

Tutuncu and Sharma (1992) measured static and dynamic Young's modulus for fully water-saturated samples. Acoustic velocities were obtained with ultrasonic pulse

transmission method and the static modulus was obtained with LVDT. Dynamic and static Young's modulus was obtained at the same stress level corresponding to in situ stress for the rocks. Tutuncu and sharma (1992) observed that the ratio between dynamic and static Young's modulus depends on the content of clay in the rock. This is in agreement with the observation for bulk modulus by Jizba et al. (1990). Tutuncu and Sharma (1992) suggest that the difference between static and dynamic Young's modulus is caused by micro cracks. Micro cracks have a larger influence on the static Young's modulus than the dynamic Young's modulus.

Tutuncu et al. (1994) worked with dry sandstone, limestones and Austin chalk and they performed loading experiments to analyze influence of strain amplitude and stress level on static Young's modulus. Static Young's modulus was obtained with strain gauges. They found that Young's modulus decreased as strain amplitude increased. For low stresses dynamic Young's modulus is higher than static Young's modulus but for increasing stress level the two moduli approaches each other.

Yale and Jamieson (1994) measured static and dynamic Young's modulus for carbonates and clastic sediments. The purpose of this study was to find a relationship between dynamic and static Young's modulus for different formations with different lithology. Based on the relationship between static and dynamic Young's modulus, static modulus can be predicted in situ based on acoustic log data for different formations in an oil reservoir. They suggest that the difference between dynamic and static Young's modulus is caused by anelastic deformation in the static measurements. Anelastic deformation does not occur in the dynamic measurements. The difference in frequency between static and dynamic measurements also has an influence on the difference between static and dynamic Young's modulus. Dynamic Young's modulus in this study is 15 %-70 % higher than static Young's modulus and the difference is largest for the softest samples.

Yale et al. (1995) measured dynamic and static Young's modulus on saturated sandstone. The ratio between dynamic and static Young's modulus depends on the porosity of the sample; for the highest porosity the ratio is around 2 and for the lowest porosity the ratio is around 1.1. The ratio between dynamic and static Young's modulus also depends on quartz cementation of the sandstone. The large amplitude in the static test causes the static modulus to be lower because of non-linear elastic deformation during static testing. Yale et al. (1995) observed only little permanent deformation for the samples, the loading and unloading curve forms almost a closed loop. In this study they also show that hysteresis is related to the difference between static and dynamic Young's modulus. The area between the loading and the unloading curve relates to the ratio between dynamic and static Young's modulus.

Plona and Cook (1995) measured static Young's modulus for dry sandstones. The test was done with a large loading cycle and smaller loading cycles during the large loading cycle. For the small loading cycle the stress was decreased 1MPa and the rock was then reloaded. After the rock was reloaded 1 MPa the rock was back on the loading curve for the large loading cycle. Static Young's modulus from the large loading cycle is 3-5 times lower than the dynamic Young's modulus. For higher stresses static Young's modulus from the small loading cycle approaches the dynamic Young's

modulus. Static Young's modulus from the minor loading cycle is equal for loading and unloading. For the large loading cycle significant hysteresis is observed and the dynamic modulus is only similar to the static modulus from the unloading curve for the highest stresses. In order to avoid influence on the static modulus from non-linear elastic deformation the static modulus should be obtained for small strains where the loading and unloading modulus is equal and similar to dynamic modulus.

Tutuncu et al. (1998) obtained static and dynamic Young's modulus for saturated sandstone. Static Young's modulus was obtained from LVDT and no permanent deformation was observed on the loading curves. The acoustic measurements were done at a frequency of 1MHz. The ratio between static and the dynamic Young's modulus was 1-6. The difference between static and dynamic Young's modulus is due to a difference in strain amplitude. They showed that if the strain amplitude increases for static test, static Young's modulus decreases.

Fjær (1999) measured static and dynamic Young's modulus for dry sandstone. Fjær (1999) suggested a model for static deformation where the deformation is a sum of an elastic deformation and a non-elastic deformation. The non-elastic deformation does not occur in dynamic measurements. The main reason for the difference between static and dynamic modulus is that failure in a rock during mechanical loading starts at low stresses before the failure is observed. This process makes the static modulus lower than the dynamic modulus.

Wang (2000) presented a large data set from different papers for soft and stiff rocks. For stiff rocks with Young's modulus above 15 GPa a good agreement between static and dynamic modulus is obtained. For softer rocks with Young's modulus less than 15 GPa a weaker agreement between static and dynamic Young's modulus was obtained. For very soft rocks the ratio between dynamic and static Young's modulus can be up to 20. Wang (2000) suggested that the difference between dynamic and static Young's modulus is caused by the difference in strain amplitude between dynamic and static measurements. In hard rocks the difference in stain amplitude does not cause a large difference between static and dynamic Young's modulus. For soft rocks the larger strain amplitude in static tests can cause non-elastic deformation during static loading which results in a lower static modulus. The difference in frequency can also cause a difference between static and dynamic Young's modulus.

Al-Tahini et al. (2004) measured static Young's modulus with LVDT and dynamic Young's modulus for dry sandstone samples. They observed that quartz overgrowth cementation for the sandstones has a large influence on the difference between static and dynamic Young's modulus.

Specific work on Danish chalk has also been done by Henriksen et al. (1999) and Gommesen and Fabricius (2001). Henriksen et al. (1999) measured dynamic Young's modulus on saturated limestone from Copenhagen and static Young's modulus with LVDT. The ratio between dynamic and static Young's modulus is 2-4. Gommesen and Fabricius (2001) worked with North Sea chalk and chalk from Ontong Java Plateau. They reported dynamic modulus based on laboratory measurements and from log data. They also obtained static oedometer modulus and bulk modulus under drained conditions. Both static oedometer modulus and bulk modulus are significantly lower

than the corresponding dynamic modulus. For the North Sea chalk samples they establish a logarithmic relationship between oedometer modulus and P-wave modulus that involves the critical porosity (Nur et al. 1998).

3.2 Dispersion

The large difference in frequency between static and dynamic measurements makes it necessary to consider if the difference in frequency may influence on Young's modulus obtained with dynamic measurements and static measurements. The acoustic velocities used to calculate dynamic Young's modulus are obtained with frequencies orders of magnitude larger than the frequency used to obtain static Young's modulus. Therefore the acoustic velocities may be higher for the frequency used in the acoustic measurements than for the frequency similar to the frequency used in the static test. Only limited knowledge about the influence of the difference between static frequency and ultrasonic frequency exists. No reliable method exists that can measure acoustic velocities continuously over several orders of magnitude of frequencies.

The influence from the frequency on the acoustic velocity is different for dry and saturated rocks. For dry rocks there is no rock physical explanation for frequency dispersion and no frequency dispersion has been reported for dry rocks below ultra sonic frequency. Spencer (1981) did not find significant frequency dispersion for dry rock. Winkler (1983) found a negative frequency dispersion of a few percent from 400 kHz to 2 MHz for sandstones; this difference is due to scattering effect at higher frequencies. For saturated rock frequency dispersion is caused by the pore fluid. Two different effects for frequency dispersion exists, the Biot flow (global flow) (Biot, 1956a, b) and squirt flow (local flow) (Mavko and Nur, 1979; Murphy et al., 1986). When an acoustic wave propagates through a porous rock with a low frequency; the pore fluid moves with the solid part of the rock. For higher frequencies the pore fluid lags behind the solid part of the rock and generates Biot flow when an acoustic wave propagates through a porous rock. This change in movement of fluid causes the acoustic velocity to be higher for high frequencies than it is for lower frequencies. Winkler (1983) did experiments with a homogeneous porous media made of fused glass beads and Berea sandstone. The media made of fused glass beads acts according to Biot's theory with a dispersion of two percent from low to high frequency. The Berea sandstone is inhomogeneous and larger dispersion then what is expected based on Biot's theory was observed for the Berea sandstone. Other studies also showed that Biot's theory does not fully explain the frequency dispersion for natural saturated rocks (Winkler, 1985; Winkler, 1986; Wang and Nur, 1988). For a natural rock the pore network is not homogenous and part of the network is more compliant than other parts of the pore network. This can cause a fluid flow from the compliant part to the less compliant part of the rock (squirt flow). For low frequency the fluid can flow and equilibrate the pressure, for high frequency the fluid does not have enough time to flow and equilibrate the pressure and the unequilibrated pressure makes the rock stiffer. For low frequency the rock is in the relaxed state and for high pressure the rock is in the

unrelaxed state. The change from relaxed to unrelaxed rock causes frequency dispersion.

Only few data exists in the literature for the size of dispersion for different reservoir rocks. Wang and Nur (1990) quantified the amount of dispersion relative to the velocity predicted with Gassmann's equation (Gassmann, 1951). Gassmann (1951) predicts velocity for saturated rock for zero frequency based on the velocity for dry rock. Wang and Nur (1990) used the measured velocity for a saturated rock at ultrasonic frequency minus the velocity calculated with Gassmanns equation divided with the Gassmann calculated velocity as a measure of velocity dispersion for saturated rocks. Wang and Nur (1990) obtained dispersions for water-saturated sandstones around 5 % for low stresses and around 2% for higher stresses. For oil-saturated sandstones the frequency dispersion was around 10% for v_p and around 8% for v_s. For water-saturated sandstones Winkler (1983) obtained similar results.

Besides Biot's model (Biot, 1956a, b) only a few models exist in the literature to calculate frequency dispersion for porous media. The model by Biot has been experimentally confirmed (Winkler, 1983). Biot flow is relatively easy to model but the squirt flow is difficult to model because it depends heavily on micro texture of the rock, the micro texture is usually not known for the rock. Because the squirt flow plays an important role in frequency dispersion (Winkler, 1985, 1986) this effect needs to be taken into consideration when the frequency dispersion is discussed and the size of it is estimated. Mavko and Jizba (1991) presented a model to calculate unrelaxed dynamic moduli based on different parameters. This model is not used in this study because it depends on parameters that can not be assessed in this study. The BISQ model estimates the p-wave velocity as a function of frequency (Dvorkin and Nur, 1993; Dvorkin et al., 1994).

The BISQ model is practical to use because it is not based on assumptions about pore geometries and it only depends on macroscopic parameters of a rock. In this model the Biot mechanism and the squirt flow is related because they both involve the pore fluid. In this report the BISQ model is only applied for frequencies below the characteristic Biot frequency.

Dvorkin and Nur (1993) predicted P-wave velocity as a function of frequency below the Biot characteristic frequency from the following equations:

$$v_p = \frac{1}{\mathrm{Re}(\sqrt{Y})} \quad (3.3)$$

$$Y = \frac{\rho_s(1-\varphi)+\rho_f\varphi}{M+F_{sq}\alpha^2/\varphi} \quad (3.4)$$

$$F_{sq} = F\left(1-\frac{2J_1(\xi)}{\xi J_0(\xi)}\right) \quad (3.5)$$

$$\xi = \sqrt{i}\sqrt{\frac{R^2\omega}{\kappa}}, \kappa = \frac{kF}{\mu\varphi} \quad (3.6)$$

$$F = \left(\frac{1}{\rho_f c_0^2} + \frac{1}{\varphi Q} \right)^{-1} \quad (3.7)$$

$$\frac{1}{Q} = \frac{1}{K_s}\left(1 - \varphi - \frac{K_{dry}}{K_s} \right) \quad (3.8)$$

$$\alpha = 1 - \frac{K_{dry}}{K_s} \quad (3.9)$$

In these equations ρ_s is the grain density, ρ_f is the fluid density, M is the dry P-wave modulus of the rock, φ is porosity, ω is the angular frequency, $J_0(\xi)$ and $J_1(\xi)$ are Bessel functions, κ is the diffusivity of the rock, k is permeability of the rock, and μ is the viscosity of the pore fluid. K_{dry} is the dry bulk modulus of the rock, K_s is the bulk modulus of the grain framework, and c_0 is the acoustic velocity of the pore fluid. R is the squirt flow length and it has the same order of magnitude as the average pore size. The physical meaning of the squirt flow length is the average length that gives a squirt flow effect identical to the cumulative effect of squirt flow in pores of various size and shape. The squirt flow length can not be measured directly but it can be obtained from matching laboratory data to the model. Another set of equations exist for frequencies above the characteristic Biot's frequency. The characteristic Biot frequency is given (Equation 3.10)

$$f_c = \frac{\varphi\mu}{2\pi\pi_{fl}k} \quad (3.10)$$

where φ is the porosity, μ is the viscosity of the pore fluid, ρ_{fl} is the fluid density and k is the permeability of the rock. The low frequency range in Biot's theory is for $f<<f_c$ and the high frequency range is for $f>>f_c$.

3.3 Drainage conditions during static loading

Static Young's modulus can be obtained for both drained and undrained conditions for porous rocks. The drained modulus is obtained when the pore fluid can flow freely out of the boundary of the sample. During a drained loading test a pressure gradient will occur in the pore fluid when the sample is loaded and the pore fluid will flow out of the sample. During a drained test the pore fluid does not contribute to the stiffness of the rock. Undrained static modulus can be obtained if the boundaries of the rock is strictly sealed of during loading of the rock and no pore fluid can escape during loading. During undrained loading the pore fluid contributes to the stiffness of the rock. The rock is therefore stiffer for undrained conditions than for drained conditions.

3.4 Marly chalk

The marly chalk (Enclosure 4 and 5) behaves differently than the clean chalk (enclosure 2 and 7) when it is deformed during a rock mechanical test. The marly chalk does not deform close to elastic as the Upper Cretaceous chalk does for low stresses. The loading curve (Figure 3.1a) shows stress vs. strain for a marly chalk sample and it is clear that it experiences non-elastic deformation during rock mechanical loading. The permanent strain increases with increasing stress for the different loading cycles. The Upper Cretaceous chalk behaves close to elastic during one loading cycle (Figure 3.1b). For the marly chalk samples the static modulus was obtained with LVDT (Linear Voltage Displacement Transducer). The loading curves from the rock mechanics test are published in a report (Christensen, 1999). The dynamic moduli are obtained from logging data. No acoustic data was obtained on the cores during rock mechanics experiments for the Lower Cretaceous samples.

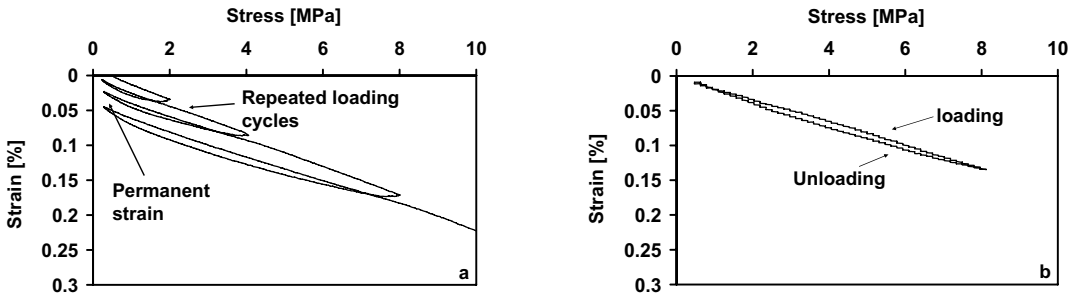

Figure 3.1 a-b. a: Loading curve for a marly chalk sample. Three loading cycles are done and the permanent strain after each loading cycle increases. b: Loading curve for an Upper Cretaceous sample .

When non-elastic deformation occurs during static loading it must influence on the static Young's modulus obtained. This kind of deformation does not occur in the dynamic measurement because of the infinitesimal small deformation. The non-elastic deformation needs to be taken into consideration when static and dynamic moduli are compared. This is normally not done in the literature, static and dynamic modulus is just compared directly. In the study on marly chalk (Enclosure 4 and 5) another approach is used where the non-elastic deformation is taken into consideration. Yale et al. (1995) observed that the ratio between static and dynamic Young's modulus is proportional to the area between the loading and unloading curve. In my study I used a more physical approach to relate static and dynamic Young's modulus. In this approach the deformation during static loading consist of an elastic and a non-elastic deformation. It was assumed that the elastic and non-elastic deformation occurs simultaneously and that the total strain increment during deformation can be formulated as a sum of an elastic strain increment and a non-elastic strain increment (Fjær, 1999; Hansen, 2001).

$$d\varepsilon = d\varepsilon_{elastic} + d\varepsilon_{non-elastic} \quad (3.11)$$

It is assumed in the model that the non-elastic deformation is controlled by stress alone. By assuming that, it is possible to rewrite Equation (3.11) to Equation (3.12).

$$\frac{1}{E} = \frac{1}{E_{elastic}} + \frac{1}{E_{non-elastic}} \quad (3.12)$$

The model (Equation 3.12) relates static Young's modulus (E), the elastic Young's modulus ($E_{elastic}$) and non-elastic Young's modulus ($E_{non\text{-}elastic}$). The elastic Young's modulus equals the dynamic Young's modulus because the dynamic modulus is obtained for a purely elastic deformation. The non-elastic deformation is described with a non-elastic modulus like the elastic deformation. The non-elastic modulus can be determined from the loading curve directly. The non-elastic modulus is obtained from the permanent deformation after each loading cycle and the maximum stress in each loading cycle (Figure 3.1a). For the different loading cycles the maximum stress vs. permanent deformation forms close to a straight line relationship and the inverse slope of the straight line is the non-elastic Young's modulus (Figure 3a). The assumption in the model (Equation 3.12) is that the elastic and the non-elastic strain increment are proportional to stress increment and that seems to be the case: The elastic strain increment in the model is derived from acoustics and thus proportional to stress. The non-elastic modulus is obtained from Figure (3.2), where a close to linear relationship between the stress and the permanent strain is observed (Figure 3.2). In this case the non-elastic strain is proportional to stress.

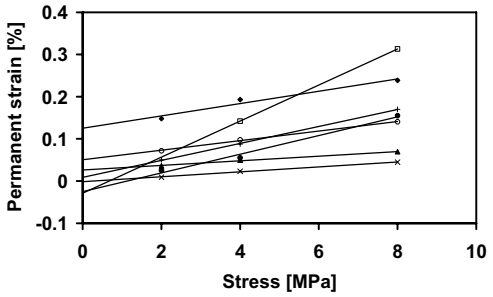

Figure 3.2. Permanent strain after each of the loading cycles versus the maximum stress in each of the three loading cycles. Strain vs. stress is approximated by a straight line and the inverse slope of the straight line defines the non-elastic modulus.

The dynamic modulus and non-elastic modulus are used to calculate the modulus for static loading (Equation 3.12). This calculated modulus compares well with the static modulus obtained from the loading curve (Figure 3.3a). The model to calculate the static modulus is very simple but it yields moduli in good agreement with the measured static moduli. The model is thus reasonable to use for calculating static Young's modulus. Comparing dynamic Young's modulus and the static measured modulus directly indicates large differences caused by the non-elastic deformation (Figure 3.3b). The non-elastic modulus can only be determined from a loading test. It is not possible based on this study to predict non-elastic Young's modulus from for example dynamic Young's and calculate static Young's modulus based on dynamic Young's modulus and a non-elastic Young's modulus for a soft sediment.

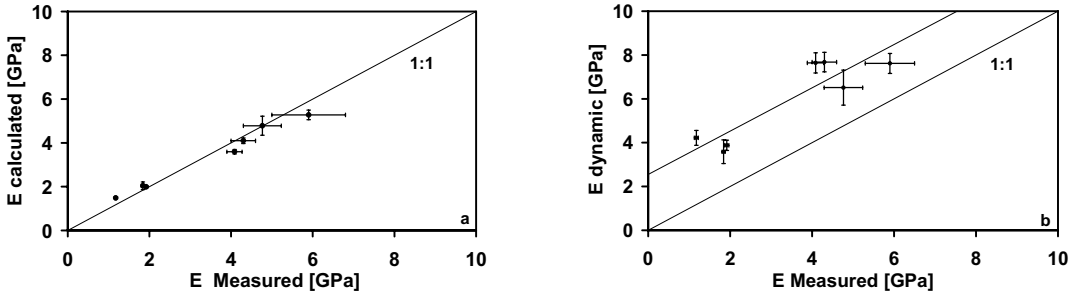

Figure 3.3a-b. a: Young's modulus calculated with Equation (3.12) vs. measured static Young's modulus obtained with LVDT from the loading curve. b: Dynamic Young's modulus vs. measured static Young's modulus obtained with LVDT from the loading curve.

In the study on the marly chalk samples only Young's modulus is discussed. It was not possible to try to establish a similar model for for example P-wave modulus and oedometer modulus, it is not possible to find out whether this approach can be used for other moduli as well. It is likely that the dynamic modulus is undrained and the static modulus is drained. If the model is to be used correctly both moduli needs to be obtained for the same drainage conditions. This is of course a weakness in the study but the approach for relating static and dynamic Young's modulus for softer rocks seems right. In this study it was not possible to try to obtain undrained static Young's modulus for the samples.

3.5 Upper Cretaceous chalk

The other part of the study on static and dynamic Young's modulus (Enclosure 2 and 7) was done on chalk samples from Upper Cretaceous formations in the North Sea. Dynamic Young's modulus in this study was obtained on the core samples in the laboratory during loading test. In this case dynamic Young's modulus is obtained for the same stress condition as static Young's modulus. Static Young's modulus is obtained in two different ways, from strain gauge and LVDT (Linear Voltage Displacement Transducer). The strain gauge is glued on the sample and it measures the deformation locally on the sample, it is not influenced by the loading frame. The LVDT is attached to the pistons during loading. The LVDT measures the deformation of the sample and the pistons. Static and dynamic Young's modulus is obtained for both dry and water-saturated samples. An undrained static test was attempted for one of the chalk samples.

The approach in this case is different than for the marly chalk samples. It is clear that only limited non-elastic deformation occurs during loading for the Upper Cretaceous sample (Figure 3.1b). The sample deforms close to linear elastic in the interval 2-5MPa where static Young's modulus is obtained. In this study it should be possible to compare static and dynamic Young's modulus with a minimum influence from non-linear elastic deformation. If non-elastic deformation is insignificant, static and dynamic Young's modulus should be equal for dry chalk. For dry chalk there should be no influence from a difference in frequency between static and dynamic

measurements. Based on the result from the dry chalk, influence of pore fluid on an apparent difference between static and dynamic Young's for water-saturated chalk can be discussed. Another central part of this study is to evaluate the two different ways of obtaining the static Young's modulus (strain gauge and LVDT).

When static Young's modulus for dry chalk obtained with strain gauge is compared to dynamic Young's modulus a good agreement is obtained (Figure 3.4a). This is expected because of insignificant influence from non-elastic deformation and frequency. Two fractured samples are included in the study; the dynamic Young's modulus is significantly larger than static Young's modulus for the fractured samples. The fractured samples do not follow the same trend line as the unfractured samples. Other studies also showed a difference in static and dynamic modulus for fractured samples (Simmons and Brace, 1965; Cheng and Johnson, 1981; Schön, 1996). Since no significant difference between static and dynamic Young's modulus for dry chalk is obtained, the results for the dry chalk is used as a reference for discussing influence of pore fluid for the water-saturated samples.

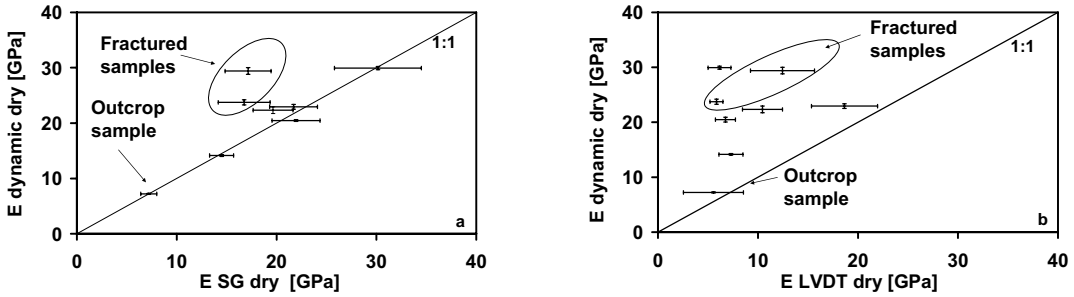

Figure 3.4a-b. Dry chalk samples. a: Dynamic Young's modulus vs. static Young's modulus based on strain gauge (SG). b: Dynamic Young's modulus vs. static Young's modulus based on LVDT.

For the water-saturated samples static Young's modulus is also obtained where the sample deforms close to linear elastic. An apparent difference between static and dynamic Young's modulus may then be caused by the pore fluid. The dynamic Young's modulus is 1.2-1.5 times larger than the apparent measured static Young's modulus based on strain gauges. The difference can be influenced both a difference in frequency and by a difference in drainage conditions. The problem about difference in frequency is discussed below. The discussion on the frequency did not show clearly how large an effect a difference in frequency has on the difference between static and dynamic Young's modulus. But the influence from frequency may by minor for North Sea chalk.

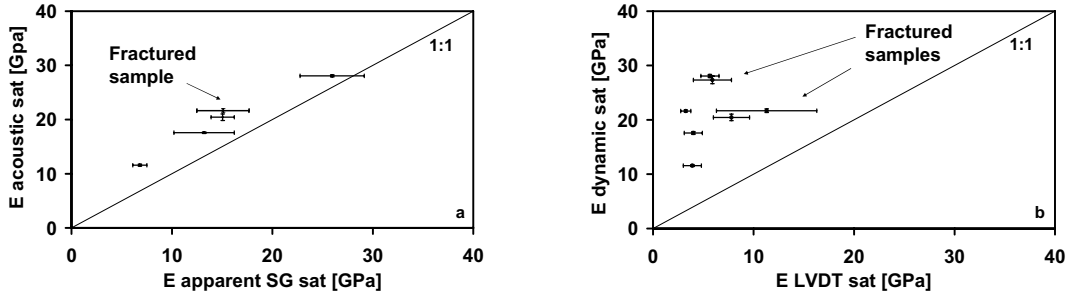

Figure 3.5a-b. Water-saturated (sat) chalk samples. a: Dynamic Young's modulus vs. apparent static Young's modulus based on strain gauge (SG). b: Dynamic Young's modulus vs. static Young's modulus based on LVDT.

During static testing the chalk sample is drained, the pore fluid is able to drain out of the sample. During dynamic measurements the pore fluid is not able to drain out of the rock and this measurement may correspond to undrained conditions. A rock is weaker for drained than for undrained conditions because the water does not contribute to the stiffness of the rock the same way for the drained and the undrained deformation. If dynamic Young's modulus is compared directly to the to static Young's modulus for water-saturated chalk two different moduli are compared and a difference between the two different moduli is observed. The static Young's modulus is therefore referred to as apparent static Young's modulus because it is not equivalent to the dynamic Young's modulus where the pore fluid influences on the stiffness of the chalk. Other effects besides difference in frequency and drainage conditions on the difference between dynamic Young's modulus and the measured apparent static Young's modulus can not be ruled out based on this study. It is not possible to say if the difference in drainage and frequency dispersion accounts for the entire difference between the dynamic Young's modulus and the measure apparent static Young's modulus.

The correct way of comparing dynamic and static Young's modulus for saturated samples is to compare dynamic Young's modulus to the undrained static Young's modulus. Undrained static modulus may be obtained for a 100% water-saturated sample where the boundaries are sealed of with an impermeable coating layer. Such a test was attempted where one of the samples was jacketed in epoxy. In order for the rock to be undrained, the end surfaces of sample as well as the cylindrical surface need to be covered with a layer of epoxy. Even though the epoxy layer on the end surfaces was only 1 mm thick, the layer had a significant influence on Young's modulus obtained. Young's modulus for the jacketed sample was around an order of magnitude lower than when the sample was not jacketed in epoxy. Therefore this kind of test should be made with a sealing material that seals off the surface of the sample without contributing to the stiffness of the rock. The sealing layer must not fracture during deformation of the rock; the advantage of using epoxy is that it does not fracture during deformation.

Another way of measuring undrained static Young's modulus is to apply a high strain rate where the pore fluid does not have enough time to escape during deformation of the rock. The main problem about applying a high strain rate is to record strain and

stress fast enough to get a sufficient amount of data points to define a loading curve. Although this approach was followed, the equipment used was not able to deform the sample fast enough to deform it undrained. The maximum strain rate for the equipment where it is be possible to record sufficient amount of stress and strain measurements is around $1.5*10^{-3}$ s^{-1} which is 500 times faster than the strain rate used in the tests performed on water-saturated samples. The stress and strain recording can only be done every second with the equipment used in this study; a loading with a strain rate of $1.5*10^{-3}$ s^{-1} took less than five seconds. The loading curve showed no sign that the chalk sample was undrained, probably because of the relative high permeability of the chalk. An undrained loading for this material might take a fraction of a second.

No clear relationship between static Young's modulus based on LVDT and dynamic Young's modulus for both dry and water-saturated samples was obtained. The ratio between dynamic Young's modulus and static Young's modulus is 1.5-7 for dry samples and 2-5 for water-saturated samples. The ratio between static Young's modulus from LVDT and dynamic Young's modulus is in agreement with other results for reservoir rocks (Tutuncu and Sharma, 1992).Since the LVDT and strain gauge gave different results for static Young's modulus it was discussed what caused this difference. Based on comparison of the absolute deformation measured with strain gauge and LVDT it turned out that the LVDT is probably more influenced by the experimental setup than the strain gauge. The LVDT is not able to accurately measure so small deformations as the deformations measured for the Upper Cretaceous samples. The strain gauge is designed to measure very small deformations accurately.

In the study on Upper Cretaceous chalk static Young's modulus based on LVDT is not related to dynamic modulus (Figure 3.4b, 3.5b) but in the study on marly chalk the static Young's modulus based on LVDT and dynamic Young's modulus are related (Figure 3.3b). For the softer marly chalk samples the difference between static and dynamic Young's modulus is caused by the non-elastic deformation during loading and not necessarily caused by an error in the LVDT measurement. The measurements for the soft marly chalk samples may be less sensitive to the errors that cause the differences between static Young's modulus based on LVDT and dynamic Young's modulus for the Upper Cretaceous samples.

3.6 Frequency

For the water-saturated Upper Cretaceous samples dynamic Young's modulus is larger than the static Young's modulus based on strain gauge. The difference in frequency between static and dynamic measurements may cause a difference between dynamic Young's modulus and static Young's modulus for water-saturated chalk. In this study it was not possible to investigate influence from frequency on acoustic velocity experimentally. Only a few observations on frequency dispersion are reported in the literature see e.g. Wang and Nur (1990) and only few models exist in the literature on frequency dispersion. Therefore it is difficult to quantify how large an

influence the difference in frequency between dynamic and static measurements has on the difference between static and dynamic Young's modulus.

In this study the BISQ model was used to investigate how acoustic velocity depends on frequency. The BISQ model only includes P-wave velocity and the model can be used both above and below Biot's characteristic frequency. In order to check whether velocity dispersion will occur due to Biot flow, the characteristic frequency for the Biot flow was calculated with Equation (3.10). For a fixed characteristic frequency the values of porosity and permeability where Biot flow will occur form a curve in a porosity permeability plot (Figure 3.6). A data set for porosity and permeability values for chalk is included in Figure (3.6). It appears that Biot flow should not occur for North Sea chalk for the frequencies used in this study (Figure 3.6).

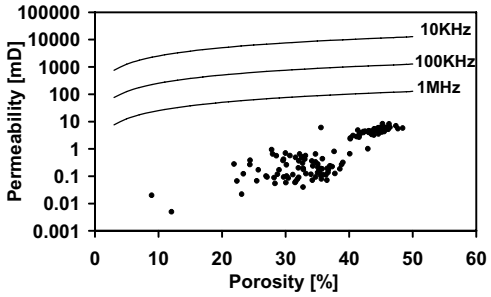

Figure 3.6. The type curves show above which permeabilities Biot flow will occur for wave frequency in kHz to the MHz region. Porosity and permeability for a set of North Sea chalk samples is included (dots).

In the BISQ model the value of R (the squirt flow length) is unknown. No data was available to match to the model in order to obtain R. R has the same order of magnitude as the pore diameter in the rock. Because it was not possible to obtain the squirt flow length the equivalent spherical pore diameter is used as an approximated squirt flow length. The equivalent spherical pore diameter can for North Sea chalk be calculated with Kozeny's equation (Equation 3.13)

$$k = c\frac{S^2}{\varphi^3} \quad (3.13)$$

Kozeny's equation can be rewritten to a relationship between equivalent spherical pore diameter, the permeability and porosity of chalk.

$$d_{eq} = \sqrt{\frac{36k}{c\varphi}} \quad (3.14)$$

where k is permeability, φ is porosity, S is specific surface with respect to bulk volume, c depends on porosity (Mortensen et al., 1998). The value of c for the porosity of the samples in this study is approx. 0.23, and d_{eq} is the equivalent spherical pore diameter (Mortensen et al., 1998).

To analyze how the frequency influences on the velocity in the BISQ model, different examples for chalk were used. For marly chalk two examples with porosity

20% and 45% and permeability of 0.07mD and 4.5mD respectively were used. For comparison an example with a sandstone from Dvorkin et al. (1994) was included. For the sandstone the squirt flow length equals 0.25mm. Two examples for Upper Cretaceous chalk was also included, the first sample has porosity 21% and permeability 0.52mD and the other sample has porosity 29% and permeability 1.83mD (Mortensen et al., 1998; Borre and Fabricius, 2001).

The P-wave velocity v_p of each of the chalk samples was calculated as a function of R and frequency. For different values of R, v_p was calculated for frequencies from zero to 1MHz. For the chalk samples values of R from 10^{-9}m to 10^{-4}m were used. v_p is constant for all frequencies up to a certain value of R, for higher values of R, the velocity starts to increase (Figure 3.7a-b)**.** For the Lower Cretaceous samples the velocity is independent on frequencies up to 1MHz when the value of R is below 10^{-5}m for 20% porosity and below 10^{-4}m for 45% porosity. The equivalent spherical pore diameter for 20% porosity is $2.4*10^{-7}$m and for porosity 45% the equivalent spherical pore diameter is $1.3*10^{-6}$m (Equation 3.14). The value of R needs to be much larger than the equivalent spherical pore diameter of the chalk to cause velocity dispersion for Lower Cretaceous chalk for frequencies below 1MHz (Figure 3.7a). This means that the marly chalk is always in the low frequency range up to 1 MHz according to the BISQ model.

For the Upper Cretaceous chalk the equivalent spherical pore diameter equals $6.2*10^{-7}$m for 21% porosity and $9.8*10^{-7}$m for 29% porosity (Equation 3.14). The value of R needs to be 10^{-4}m before the velocity depends on frequency when the porosity is 29% and when the porosity is 21% only a slight increase in velocity occurs when R equals 10^{-5} (Figure 3.7b). According the the BISQ model the Upper Cretaceous chalk is in the low frequency range below 1MHz. This means that the acoustic P-wave velocity is the same for static low frequency measurements and dynamic high frequency measurements according to the BISQ model.

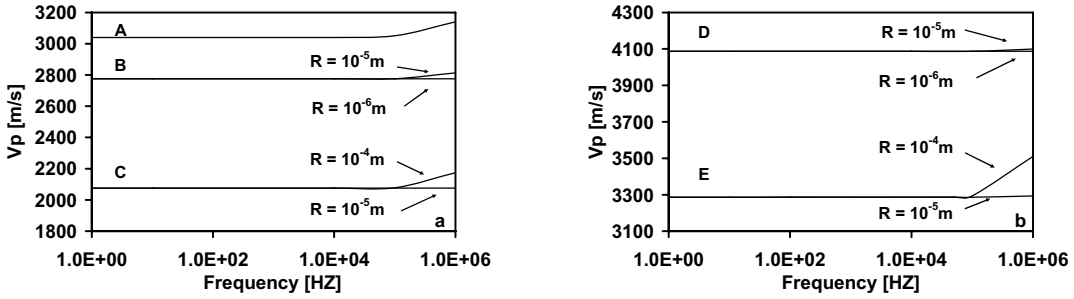

Figure 3.7a-b. v_p as a function of frequency for different values of R according to the BISQ model. a: A is sandstone sample from Dvorkin et al. (1994), B is the sample with 20% porosity and permeability 0.07mD, and C is the sample with 45% porosity and permeability 4.5mD. B and C are Lower Cretaceous samples. b: velocity for Upper Cretaceous samples. Sample D has 21% porosity and permeability 0.52mD and sample E has porosity 29% and permeability 1.83mD.

The result from the analysis of the BISQ model is weak. The model is based on a heuristic parameter, the squirt flow length. It is assumed in the model that the squirt

flow length has the same order of magnitude as the diameter of the pores in the porous medium. The squirt flow length is difficult to determine. No data was available to match to the model in order to obtain squirt flow length. It was just assumed that the squirt flow length has the same order of magnitude as the equivalent spherical pore diameter and that the squirt flow length could be approximated with the equivalent spherical pore diameter. This model is a simple way of evaluating frequency dispersion. The analysis of this model is only included in this study because it was the only model available.

The results from the analysis of the BISQ model and the few data in the literature about frequency dispersion do not give an answer to how large the frequency dispersion is for chalk. It is therefore not possible to determine how large a part of the difference between static and dynamic Young's modulus for water-saturated chalk that possible may be caused by frequency dispersion. But other research results have indicated that the chalk may be in the relaxed state even for ultra sonic frequencies (Røgen et al., 2005). Røgen et al. (2005) found that sonic velocities measured on dry chalk matched sonic velocities calculated from sonic velocities obtained for water-saturated samples using Gassmann's equations (Gassmann, 1951). If the low frequency model by Gassmann (1951) is applicable to chalk it could indicate that the chalk is in the low frequency range for ultrasonic velocity. In that case the acoustic velocity obtained at static low frequency interval equals the acoustic velocity measured at ultra sonic frequency.

The two different studies on static and dynamic Young's modulus are therefore important for relating static and dynamic Young's modulus. The marly chalk study is done on samples with a clear non-elastic deformation during loading and in this case the deformation can be described as a sum of an elastic and a non-elastic deformation. The non-elastic deformation is characterized with a non-elastic modulus and this non-elastic modulus can be obtained directly from the loading curve. When the non-elastic modulus is taken into consideration, the static and dynamic Young's modulus can be related through a model including the static Young's modulus, the elastic Young's modulus and the non-elastic Young's modulus. In the study on Upper Cretaceous chalk the samples are so cemented and stiff that non-elastic deformation is insignificant. Static Young's modulus from the loading curve is obtained where the sample deforms close to linear elastic. In this case the static Young's modulus equals the dynamic Young's modulus for dry chalk where no significant influence from the pore fluid occurs. For water-saturated chalk a difference is observed between static and dynamic Young's modulus probably caused by the pore fluid.

An interesting aspect is why this large non-elastic deformation occurs for the marly chalk samples and not for the Upper Cretaceous chalk samples. The non-elastic deformation must be related to movements of the grains in the rock. The grains can only move relatively to each other permanently if they are not glued together by cement. The marly chalk samples may be less cemented because of the content of clay in the samples. The Upper Cretaceous samples are cemented and in this case the static and dynamic Young's modulus is equal for dry chalk. For comparison Al-Tahini et al. (2004) studied sandstone samples and observed that cementation has a large effect on

the difference between static and dynamic Young's modulus. Samples with quartz overgrowth cement had a lower difference between static and dynamic Young's modulus than samples with no overgrowth cement. Yale et al. (1995) also reported that the ratio between static and dynamic Young's modulus is dependent on overgrowth cementation. It was in this study not possible to make a further discussion for the samples in relation to cementation.

4. Archie's cementation factor

Archie's cementation factor (Archie, 1942) is central for determining fluid saturations in a hydrocarbon reservoir. If a wrong cementation factor is used, it can lead to wrong prediction of fluid saturations and wrong reserve estimations (Borai, 1987). Further discussion of variations in cementation factor for chalk and other reservoir rocks and possible relationships between the cementation factor and other physical properties of reservoir rocks is of interest. A relationship between electric properties and acoustic properties of a reservoir rock may be interesting for different reasons. In the last decade more attention has been given to combing seismic methods and EM methods in hydrocarbon exploration. Recent studies have shown benefit of combining seismic and EM methods (Hoversten et al., 2003; Zhanxiang et al., 2007). Combining elastic properties and electric properties can also be used in log interpretation as suggested by Faust (1953) and further discussed by Hacikoylu et al. (2006). They suggested that acoustic velocities could be predicted from formation factor, because formation factor and acoustic velocity both dependent on porosity and therefore must to some extent be related. Another possible application is to predict cementation factor from acoustic logs and use it for fluid saturation calculation.

In this study it is analyzed which physical properties control the cementation factor for porous reservoir rocks. It is also discussed if it is possible to related cementation factor to elastic properties through Biot's coefficient.

Archie (1942) introduced a simple relationship (Equation 4.1) between the resistivity of a porous rock and the porosity of the rock

$$F = \frac{1}{\varphi^m} \quad (4.1)$$

where F is formation factor, φ is porosity and m is Archie's cementation factor. The equation only applies to sediments where the electrical current is carried by an electrolytic pore fluid and the grains are insulators. The formation factor is defined in Equation (4.2) where R_o is resistivity of brine-saturated rock and R_w is resistivity of the brine.

$$F = \frac{R_o}{R_w} \quad (4.2)$$

Even though the cementation factor is a central parameter for calculation of fluid saturations and hydrocarbon reserves, only little work has been done to discuss the cementation factor and how it depends on other rock properties. The cementation factor was introduced by Archie (1942) where a large number of sandstone samples were measured. Archie obtained cementation factors in the interval 1.8-2.0 and Archie (1942) postulated that the cementation factor depends on degree of cementation for porous

rocks. Other authors have presented results about the cementation factor (Wyllie and Gregory; Jackson, 1978; Borai, 1987; Focke and Munn, 1987; Saha et al., 1993; Ragland, 2002).

A variation in cementation factor with porosity has been reported (Borai, 1987; Focke and Munn, 1987, Saha et al., 1993). Borai (1987) presented a study on carbonates from the Middle East. Borai (1987) observed a clear decrease in cementation factor with decreasing porosity. The cementation factor varied from above 2 for porosities above 15% and down to 1.5 for porosities around 3%. Focke and Munn (1987) obtained results similar to Borai (1987); the highest values for the cementation factor was around 2 for porosity in the interval 8 % to 30 % and cementation factor is significantly lower than 2 for lower porosities. Saha et al. (1993) measured cementation factor in the interval 1.48 to 2.45 for dolomites. The cementation factor decreased with porosity in the porosity interval 3 % to 29 %. Cementation factor has also been reported to depend on pore type (Focke and Munn, 1987; Ragland, 2002). Cementation factor in the interval 2 to 5.4 was reported by Focke and Munn (1987) for moldic limestones. For carbonates with interparticle porosity the cementation factor is also influenced by other pore types (Ragland, 2002). She found cementation factors in the interval 1.29-3.23.

In this study I focused on North Sea chalk with interparticle porosity. A variation in cementation factor for sediments with interparticle porosity was related to the shape of the grains (Wyllie and Gregory, 1953; Jackson et al., 1978). Wyllie and Gregory (1953) found that for the same porosity the cementation factor is lowest when the grains are spherical, other grain shapes such as discs, cubes, and triangular prisms had higher cementation factor. The difference in cementation factor between spheres and non-spheres was up to 20 %. Similarly Jackson et al. (1978) found that the cementation factor depends on shape of particles. The cementation factor varied from 1.2 for spheres to 1.9 for platy shells fragments for unconsolidated sediments. Variation in size and sorting of the grains had less influence on the cementation factor.

Several studies related electric properties to acoustic properties of sediments (Faust, 1953;; Shang et al., 2005, Hackikoylu, 2006; Gommesen et al., 2007). The first attempt to relate electric properties and acoustic properties was done by Faust (1953). He presented an equation that relates P-wave velocity, v_p, formation factor, and depth. This equation could be used to construct a velocity curve from a resistivity curve where velocity data were missing or of bad quality. Hacikoyle et al. (2006) applied the equation by Faust (1953) to sand and shale in order to make a transform between resistivity and acoustic velocity based on a rock physics model. Shang et al. (2005) related elastic properties to electric properties through an equivalent rock element model, where the formation factor was computed based on porosity, bulk modulus and shear modulus. Gommesen et al. (2007) showed that Biot's coefficient, porosity and cementation factor is related for North Sea chalk based on water zone logging data and that cementation factor decreases with decreasing Biot's coefficient.

4.1 Predicting cementation factor

Based on the studies on variation in cementation factor and possible relationships between electric properties and acoustic properties, it is clear that further studies on the cementation factor is needed. Several studies have shown variation in cementation factor with porosity (Borai, 1987; Focke and Munn, 1987, Saha et al., 1993) and other studies have shown a variation in cementation factor with grain shape (Wyllie and Gregory, 1953; Jackson et al., 1978). Because a variation in cementation factor related to both a variation in porosity and grain shape is observed, it would be interesting to discuss cementation factor versus specific surface.

The main result from the study on Archie's cementation factor is a relationship between cementation factor and specific surface with respect to bulk volume (Figure 4.1a). It has not been directly reported before by other researchers. The specific surface is with respect to bulk volume because the electric property is obtained for the bulk volume of the rock. The relationship is in agreement with the results by other studies (Wyllie and Gregory, 1953; Jackson et al., 1978) where the cementation factor depends on grain shape. The specific surface is related to the grain shape because the specific surface is the surface area of the grains normalized to either the mass or the volume of the rock.

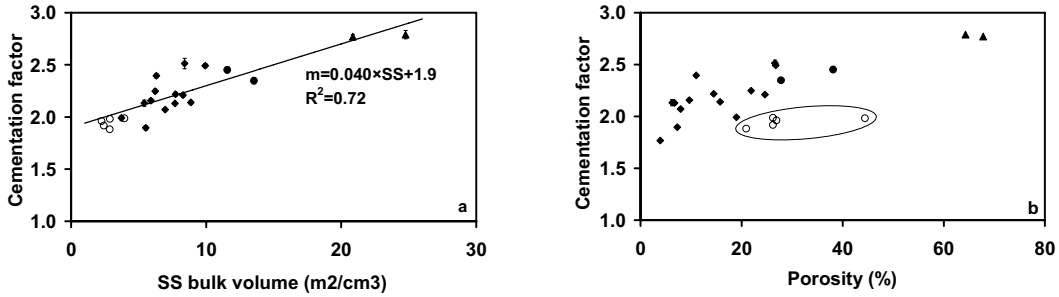

Figure 4.1 a-b. a: Cementation factor vs. specific surface (SS) for bulk volume of chalk. b: Cementation factor vs. porosity. The Nana and Stevns outcrop samples are marked on the figure with an ellipse, these samples have low specific surface. Filled dots are Valhall samples, triangles are ODP (Ocean Drilling Project) samples, the open dots are Nana and Stevns outcrop samples and filled diamonds are samples from Fabricius et al. (in press).

Cementation factor is not directly controlled by the porosity (Figure 4.1b). If the data are divided into two groups, a more clear relationship between cementation factor and porosity is obtained. This is done because the group marked with an ellipse (Figure 4.1b) has lower specific surface than the other samples. The cementation factor is in this study up to around 2.5 for the North Sea samples and around 2.8 for the ODP (Ocean Drilling Project) samples. The cementation factor is high when the specific surface is high (Figure 4.1a). A high specific surface may be related to the content of fine grained silica in the chalk samples. Silica has a significant influence on specific surface for North Sea chalk (Røgen and Fabricius, 2002); therefore cementation factor is compared

to carbonate content (Figure 4.2). For North Sea chalk content of silica is directly related to the content of carbonate (Røgen and Fabricius, 2002). It seems like the cementation factor depends on the silica content, the cementation factor in general increases as the carbonate content decreases but the relationship is scattered (Figure 4.2). The relationship between specific surface and cementation factor is a more interesting result because it puts the cementation factor into a context with the physics of chalk and not only geological aspects of chalk. It was in this study not possible to directly discuss influence from cementation on the cementation factor. Cementation will change the smoothness of the grains and the specific surface but because of a variation in content of fine grained silica the influence of the smoothness of the calcite grains can not be studied directly.

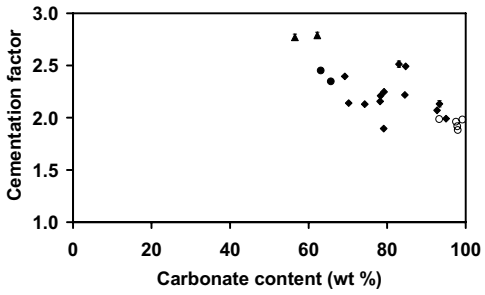

Figure 4.2. Cementation factor vs. content of carbonate in solid phase in the chalk samples. Filled dots are Valhall samples, triangles are ODP (Ocean Drilling Project) samples, the open dots are Nana and Stevns outcrop samples and filled diamonds are samples from Fabricius et al. (in press).

Based on the relationship between specific surface and cementation factor an interesting application arises. The specific surface with respect to bulk volume is usually not known for reservoir rocks because it is often not measured. Kozeny's equation (Equation 4.3) relates liquid permeability, porosity and specific surface with respect to bulk volume

$$k = c\frac{\varphi^3}{S^2} \quad (4.3)$$

where k is liquid permeability, φ is porosity and S is specific surface with respect to bulk volume. Mortensen et al. (1998) showed that permeability for chalk can be predicted based on porosity and specific surface. Permeability and porosity are usually known for reservoir rocks. The relationship between specific surface and cementation factor would be interesting from an applied point of view if the specific surface could be predicted from porosity and permeability.

Specific surface with respect to bulk volume was calculated from Kozeny's equation based on porosity and permeability for the chalk samples used in this study. The method was also applied to sandstones from a study by Raiga-Clemenceau (1977). For the sandstone samples the cementation factor was calculated based on Equation 4.1. The cementation factor vs. predicted effective specific surface forms a common log-linear relationship for chalk samples and sandstone samples (Figure 4.3). The samples

with an effective specific surface with respect to bulk volume area higher than 1 m^2/cm^3 are chalk samples and the samples with an effective specific surface area with respect to bulk volume lower than 1 m^2/cm^3 are sandstone samples from Raiga-Clemenceau (1977). The permeability of the sandstones in Raiga-Clemenceau (1977) is orders of magnitude larger than the permeability of North Sea chalk; therefore the effective specific surface with respect to bulk volume is much lower than for North Sea chalk. The samples with a specific surface around 1 m^2/cm^3 have a cementation factor around 2 which is common for carbonates. If the specific surface deviates significantly from 1 m^2/cm^3 then the cementation factor deviates from 2. In this case the specific surface is the effective specific surface. For sandstones small fractures occurs on the surface of the grains. The surface area of the small fractures does not contribute to the specific surface that controls permeability. Chalk grains have a smooth surface where small fractures in the grains do not occur as they do for the grains in the sandstone. Therefore the measured specific surface in the laboratory corresponds to the effective specific surface controlling permeability for chalk. The specific surface for sandstone measured in the laboratory does not correspond to the specific surface controlling permeability for sandstones because of the surface area in the fractures contributes to the specific surface measured in the laboratory. Therefore Kozeny's equation does not work for sandstones to predict permeability from porosity and specific surface measured in the laboratory (Solymar, 2002). Kozeny's equation can be used to predict the effective specific surface for sandstones based on porosity and permeability because the permeability is only influenced by the effective specific surface of a sediment.

Chalk and sandstones are often treated in different ways when Archie's equation is used. Based on Figure 4.3 it seems like sandstones and chalk can be treated equally when Archie's equation is used to calculate fluid saturations. They follow the same trend line when cementation factor is discussed versus specific surface with respect to bulk volume and the specific surface with respect to bulk volume controls the cementation factor.

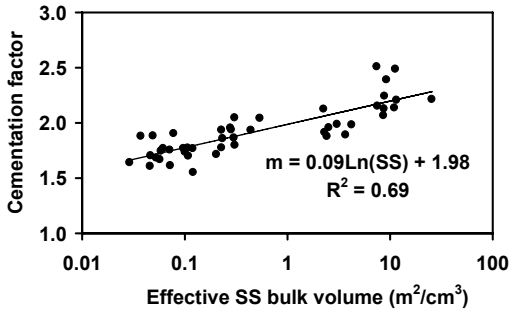

Figure 4.3. Cementation factor vs. effective specific surface calculated with Kozeny's equation based on porosity and permeability. Samples with effective specific surface larger than 1 m^2/cm^3 are chalk samples and samples with an effective specific surface less than 1 m^2/cm^3 are sandstone samples from Raiga-Clemenceau (1979).

4.2 Relating electric properties to elastic properties of chalk

When cementation factor is compared to acoustic properties Biot's coefficient is used. The relationship between cementation factor and Biot's coefficient is negative and

vague (Figure 4.4a). The vague relationship may be caused by the influence from the content of silica in the chalk. The content of silica will contribute to the specific surface and therefore influence on the cementation factor. The silica will not contribute to the stiffness of the grain contacts and it will therefore not influence the same way on Biot's coefficient as it will on the cementation factor.

The cementation factor is also discussed in relation to other elastic properties of chalk v_p/v_s, poisson's ratio and p-wave velocity and shear wave velocity of dry chalk (Figure 4.4b-e). For v_p/v_s and poisson's ratio for dry chalk the data is so scattered that a relationship between cementation factor and the elastic properties does not exist. The relationship between v_p and v_s and the cementation factor is less scattered.

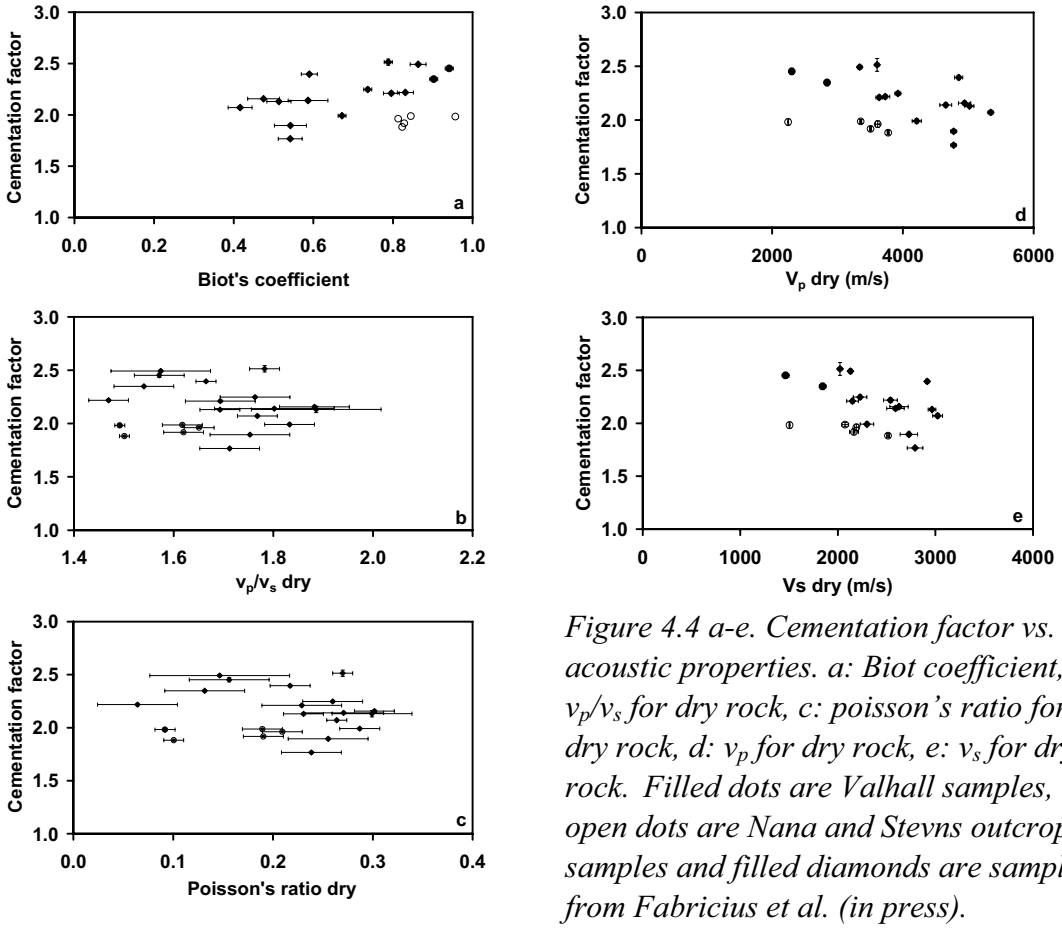

Figure 4.4 a-e. Cementation factor vs. acoustic properties. a: Biot coefficient, b: v_p/v_s for dry rock, c: poisson's ratio for dry rock, d: v_p for dry rock, e: v_s for dry rock. Filled dots are Valhall samples, open dots are Nana and Stevns outcrop samples and filled diamonds are samples from Fabricius et al. (in press).

The relationships between the cementation factor and the elastic properties can not be used to make an accurate prediction of the cementation factor based on elastic properties because of the large scatter in the plots. A relationship between acoustic properties and cementation factor is not straight forward. The elastic properties are primarily dependent on the stiffness of the grain contacts and the cementation factor is primarily dependent on the specific surface with respect to bulk volume of the rock. The specific surface and grain contact stiffness are both dependent on degree of cementation

but a variation in the content of silica has a large influence on specific surface but not on the grain contact stiffness.

5. Conclusions

Biot's coefficient can be used as a measure of degree of cementation for pure North Sea chalk with a calcite content of more than 95%.

The Iso-Frame model and the BAM model predict P-wave modulus and shear modulus with some inconsistencies for dry and water-saturated chalk. The models are most consistent between P-wave modulus for dry and water-saturated chalk and the models are least consistent between dry and water-saturated shear modulus. Dvorkin's cemented sand model is only consistent for the softest chalk samples in this study and it is only applicable to dry rock. Berryman's cemented sand model is consistent between P-wave modulus and shear modulus for one pore fluid but it is not consistent between dry and water-saturated chalk.

The free parameter in the Iso-Frame model, the BAM model and Dvorkin's cemented sand model is related to Biot's coefficient or pore space compressibility. For Berryman's self-consistent model the free parameter is only related to Biot's coefficient for water-saturated chalk when the aspect ratio for the grains and the pores are equal.

The Iso-Frame model and the BAM model predicts Biot's coefficient based on P-wave velocity and density for water-saturated chalk better than Berryman's self-consistent model.

Overall the Iso-Frame model and the BAM model are better to use for chalk than Berryman's self-consistent model and Dvorkin's cemented sand model.

For the less cemented Lower Cretaceous marly chalk samples dynamic and static Young's modulus are different due to a significant non-elastic deformation during static deformation. For the Lower Cretaceous samples a model is proposed to relate static and dynamic Young's modulus when non-elastic deformation occurs during static loading. In this model inverse static Young's modulus equals the sum of inverse elastic Young's modulus and inverse non-elastic Young's modulus. The non-elastic deformation during static loading is described with a non-elastic modulus and a method of assessing non-elastic modulus from permanent strain after each loading cycle is suggested. Static Young's modulus predicted with this model is in agreement with the static Young's modulus obtained from the loading curve.

For the Upper Cretaceous samples static Young's modulus for dry chalk obtained from strain gauge equals dynamic Young's modulus. The sample deforms close to linear elastic and there is no influence from the strain amplitude on Young's modulus obtained.

For the water-saturated Upper Cretaceous samples dynamic Young's modulus is larger than the apparent static Young's modulus obtained with strain gauge in the stress interval where the samples deform close to linear elastic. The difference between apparent static Young's modulus and dynamic Young's modulus for water-saturated chalk may be caused by a difference in drainage conditions between static and dynamic measurements and an influence from difference in frequency between static and dynamic measurements may also play a role. It was not possible to prove that the

influence from difference in drainage conditions and influence from frequency can fully explain the difference between static and dynamic moduli; other effects can not be ruled out. For water-saturated rock dynamic Young's modulus should be compared to undrained static Young's modulus. It was not possible to obtain undrained static Young's modulus in this study.

Static Young's modulus obtained from LVDT for Upper Cretaceous chalk is not related to dynamic Young's modulus. The LVDT is influenced by the experimental setup and it makes the LVDT inaccurate to use for measuring small strains like the strains for the samples in this study.

For chalk Archie's cementation factor varies and it is primarily controlled by the specific surface with respect to bulk volume of chalk. An apparently linear relationship between Archie's cementation factor and specific surface with respect to bulk volume was obtained. Archie's cementation factor is also related to the porosity of the rock but a large scatter is observed in the relationship between Archie's cementation factor and porosity due to a variation in specific surface for chalk.

A vague relationship between Archie's cementation factor and Biot's coefficient was obtained were Archie's cementation factor decreases for decreasing Biot's coefficient. The reason for the vague relationship is probably a variation in the content of non-carbonate in the chalk.

For the chalk samples in this study and for sandstones from a published study a common log-linear relationship was obtained between Archie's cementation factor and the effective specific surface obtained through Kozeny's equation and porosity and permeability.

6. Manuscript abstracts

Abstract from manuscript 1

In this study we predict Biot's coefficient for North Sea chalk based on density and P-wave velocity for water-saturated chalk. We compare three different effective medium models: Berryman's self-consistent model, the Iso-Frame model and the bounding average method (BAM). The self-consistent model is used with two different combinations of aspect ratios; one where the aspect ratio is equal for pores and grains and one where the aspect ratio for the grains is kept constant close to one and the aspect ratio for the pores varies. All the models include one free parameter that determines the stiffness of the rock for a fixed porosity. This free parameter is compared to Biot's coefficient to discuss if the free parameter is related to pore space compressibility for North Sea chalk. We also discuss how consistent the models are between P-wave modulus and shear modulus for dry and water-saturated chalk. The acoustic velocity and the density data for dry and water-saturated chalk are all laboratory data. The Iso-Frame model and the BAM model predicts Biot's coefficient with a smaller error than the self-consistent model. The free parameter in the Iso-Frame model and the BAM model is related to Biot's coefficient. The free parameter in the self-consistent model is only related to Biot's coefficient for water-saturated chalk when the aspect ratio for the pores and the grains are equal. The Iso-Frame and the BAM model are in general more consistent for chalk than the self-consistent model.

Abstract from manuscript 2

In this paper we present results from a study on dynamic and static Young's modulus of North Sea chalk. All moduli are obtained based on laboratory methods for both dry and water-saturated chalk. The static moduli are obtained with strain gauge and LVDT (Linear Voltage Displacement Transducer). Influence of pore fluid on static and dynamic Young's modulus is discussed and the two different methods for obtaining static Young's modulus are evaluated. We obtain a good agreement between dynamic Young's modulus and strain gauge static Young's modulus for dry chalk but for water-saturated chalk, the dynamic Young's modulus is larger than the apparent static Young's modulus. The difference between apparent static and dynamic Young's modulus for water-saturated chalk is explained by a difference in drainage conditions although other effects cannot be ruled out. One perspective of the difference between drained and undrained water-saturated Young's modulus is to explain why chalk oil fields deform during water injection. When water injection begins, the chalk and the water phase change from undrained to drained conditions and it causes the chalk field to become weaker. Dynamic dry Young's modulus is larger than dynamic water-saturated Young's modulus maybe due to shear weakening of the chalk when it is water-saturated. The difference between dry and water-saturated modulus is larger for static modulus than for dynamic modulus. In the static case the difference is caused both by a difference in drainage conditions and shear weakening of the water-saturated chalk. The weakening effect may also be larger for larger strain amplitude. Young's modulus from

LVDT measurements does not relate to dynamic Young's modulus for dry or water-saturated rock. This is because the LVDT is influenced by the experimental setup. The LVDT is not able to accurately measure the small deformations the samples experience during loading at relatively low stresses.

Abstract from manuscript 3

Based on Archie's cementation factor as measured on North Sea chalk and on published data we discuss how the cementation factor depends on other physical properties of the chalk. A relationship between cementation factor and specific surface with respect to bulk volume was obtained for chalk. This leads to a discussion of how Archie's cementation factor may be predicted from porosity and permeability for chalk as well as for sandstone.

Biot's coefficient and the cementation factor both depend on degree of cementation of chalk, but we found that whereas cementation factor primarily depends on the smoothness of all particles as described by the specific surface, Biot's coefficient is closely related to the stiffness of the grain contacts. Both the smoothness of the grains and the stiffness of the grain contacts depend on cementation, but for chalk only a vague negative relationship between Biot's coefficient and cementation factor was obtained. This vagueness in the relationship is caused by a variation in content of fine grained silica, the silica has a large influence on specific surface of the chalk and the cementation factor but it does not have a significant influence on the grain contact stiffness and Biot's coefficient.

7. References

Al-Tahini, A. M., C. H., Sondergeld, and C. S. Rai, 2004, The effect of cementation on static and dynamic properties in Jauf and Unayzah formations at Saudi Arabia: SPE Annual Conference and Exibition, SPE, SPE number 90448.

Archie, G. E., 1942, The electrical resistivity log as an aid to determining some reservoir characteristics: Transactions of the American Institute of Mining and Metallurgical Engineers, **146**, 54-62.

Berryman, J. G., 1980, Long-wavelength propagation in composite elastic media II. Ellipsoidal inclusions: Journal of the Acoustic Society of America, **68**, 1820-1831.

Biot, M. A., 1956a, Theory of propagation of elastic waves in a fluid saturated porous solid. I. low-frequency range: Journal of Acoustical Society of America, **28**, 168-178.

Biot, M. A., 1956b, Theory of propagation of elastic waves in a fluid saturated porous solid. II. high-frequency range: Journal of Acoustical Society of America, **28**, 179-191.

Biot, M. A., and D. G. Willies, 1957, The elastic coefficients of theory of consolidation: Journal of Applied Mechanics, **24,** 594-601.

Borre, M. K., and I. L. Fabricus, 1998, Chemical and mechanical processes during burial diagenesis of chalk: an interpretation based on specific surface data of deep-sea sediments: Sedimentology, **45**, 755-769.

Borre, M. K., and I.L. Fabricius, 2001, Ultrasonic velocities of water saturated chalk from the Gorm field, Danish North Sea: Sensitivity to stress and applicability of Gassmann's equation, in I. L. Fabricius eds., Nordic Petroleum Technology Series Nordisk Energiforsknings Program, **V**, 1-18.

Borai, A. M., 1987, A new correlation for the cementation factor in low-porous carbonates: SPE Formation Evaluation, June, 495-499. SPE number 14401.

Brandt, H., 1955, A study of the speed of sound in porous media: Journal of applied Mechanics, **22**, 479-486.

Budiansky, B., 1965, On the elastic moduli of some of heterogeneous materials: Journal of Mechanics and Physics Solids, **13**, 223-227.

Cheng, C. H., and D H. Johnson, 1981, Dynamic and static moduli: Geophysical Research Letters, **8**, 39-42.

Christensen, C. T., 1999, Rock mechanical properties - Lower Cretaceous, Valdemar: Danish Energy Agency, Copenhagen, Denmark.

Cleary, M. P., I. W. Chen, and S. M. Lee, 1980, Self-consistent techniques for heterogeneous media: American society of civil engineering Journal Engineering Mechanics, **106**, 861-887.

Digby, P. J., 1981, The effective elastic moduli of porous granular rocks: Journal Applied Mechanics, **48**, 803-808.

Dvorkin, J., and A. Nur, 1993, Dynamic poroelasticity: A unified model with the squirt and the Biot mechanism: Geophysics, **58**, 524-533.

Dvorkin, J., R. N. Hoeksema, and A. Nur, 1994, The squirt-flow mechanism: Macroscopic description: Geophysics, **59**, 428-438.

Dvorkin, J., A. Nur, H.Yin, 1994, Effective properties of cemented granular materials: Mechanics of Materials, **18**, 351-366.

Dvorkin, J., M. Prasad, A. Sakai, and D. Lavoie, 1999, Elasticity of marine sediments: Rock physics modeling, Geophysical Research Letters, **26**, 1781-1784.

Fabricius, I. L., 2003, How burial diagenesis of chalk sediments controls sonic velocity and porosity: AAPG Bulletin, **87**, 1-24.

Fabricius, I.L., C. Høier, P. Japsen, and U. Korsbech, 2007, Modeling elastic properties of impure chalk from the South Arne field, North Sea: in press Geophysical Prospecting.

Faust, L. Y., 1953, A velocity function including lithologic variations: Geophysics, **18**, 271-288.

Fjær, E., 1999, Static and dynamic moduli for weak sandstones, *in* B. Amadei, R. L. Kranz, G. A. Scott, and P. H. Smeallie, eds, Rock mechanics for industry, Balkema, 675-681.

Fjær, E., R. M. Holt, P. Horsrud, A. M. Raaen, and R. Risnes, 1992, Petroleum related rock mechanics, Developments in petroleum science **(33)**: Elsevier.

Focke, J. W., and D. Munn, 1987, Cementation exponents in Middle Eastern carbonate reservoirs: SPE Formation Evaluation, **2**, 155-167.

Gassmann, F., 1951, Über die elastizitat poroser medien: Verteljahrsschrift der Naturforshenden Gesellschaft in Zurich, **96**, 1-23.

Geertsma, J., 1957, The effect of fluid pressure decline on volumetric changes of porous rocks: Petroleum Transactions of AIME, **210**, 331-340.

Gommesen, L., and I. L. Fabricius, 2001, Dynamic and static elastic moduli of North Sea and deep sea chalk: Physics and Chemistry of the Earth Part A-Solid Earth and Geodesy, **26**, 63-68.

Gommesen, L., I. L. Fabricius, T. Mukerji, G. Mavko, and J. M. Pedersen, 2007, Elastic behaviour of North Sea chalk, A well log study: Geophysical prospecting, **55**, 307-322.

Hacikoylu, P., J. Dvorkin, and G. Mavko, 2006, Resistivity-velocity transforms revisited: The Leading Edge, **25**, 1006-1009.

Hansen, B, 2001, Advanced theoretical soil mechanics, dgf-Bulletin Danish Geotechnical Society.

Hashin, Z., and S. Shtrikman, 1963, A variational approach to the elastic behaviour of multiphase materials: Journal of Mechanics and Physics Solids, **11**, 127-140.

Henriksen, A. D., I. L. Fabricius, M. K. Borre, U. Korsbech, A. T. Theilgaard, J. B. Zandbergen, 1999, Core density scanning, degree of induration and dynamic elastic moduli of Palaeogene limestone in the Copenhagen area: Quarterly Journal of Engineering Geology, **32**, 107-117.

van Heerden, W. L., 1987, General Relatios between static and dynamic moduli of rocks: International Journal of Rock Mineral Science and Geomechanical Abstracts, **24**, 381-385.

Hertz, H., 1882, Über die berührung fester elastischer körper (On the contact of elastic solids): Journal reine und angewandte Mathematik, **92**, 156-171.

Hill, R., 1965, A self-consistent mechanics of composite materials: Journal of Mechanics and Physics Solids, **13**, 213-222.

Hoversten, G. M., R. Gritto, J. Washbourne, and T. Daley, 2003, Pressure and fluid saturation prediction in a multicomponent reservoir using combined seismic and electromagnetic imaging: Geophysics, **68**, 1580-1591.

Jackson, P. D., D. Taylor-Smith, and P. N. Stanford, 1978, Resistivity-porosity-particle shape relationships for marine sands: Geophysics, **43**, 1250-1268.

Jizba, D., G. Mavko, and A. Nur, 1990, Static and dynamic moduli of tight gas sandstones: 60st Annual International Meeting, SEG, Expanded Abstracts, 827-829.

Kieffer, S. W., 1977, Sound speed in liquid-gas mixtures: Water-air and water-steam: Journal of Geophysical Research, **82**, 2895-2904.

Kuster, G. T., and M. N. Toksöz, 1974, Velocity and attenuation of seismic waves in two-phase media: Geophysics, **39**, 587-618.

Marion, D., 1990, Acoustic, mechanical and transport properties of sediments and granular materials: PhD dissertation, Stanford University.

Mavko, G., and D. Jizba, 1991, Estimating grain-scale fluid effects on velocity dispersion in rocks: Geophysics, **56**, 1940-1949.

Mavko, G., T. Mukerji, and J. Dvorkin, 1998, The rock physics handbook: Cambridge University Press.

Mavko, G., and A. Nur, 1979, Wave attenuation in partially saturated rocks: Geophysics, **44**, 161-178.

Mindlin, R. D., 1949, Compliance of elastic bodies in contact: Journal of Applied Mechanics, **16**, 259-268.

Mortensen, J., F. Engstrøm, and I.L. Fabricius, 1998, The relation among porosity, permeability, and specific surface of chalk from Gorm field, Danish North Sea: SPE Reservoir Evaluation & Engineering, **June**, 245-251.

Montmayeur, H., R. M. Graves, 1985, Prediction of static elastic/mechanical properties of consolidated and unconsolidated sands from acoustic measurements: 60th Annual Technical Conference and Exhibition, Society of Petroleum Engineers, SPE 14159.

Mukerji, T., J. G. Berryman, G. Mavko, and P. A. Berge, 1995, Differential effective medium modeling of rock elastic moduli with critical porosity constraints: Geophysical Research Letters, **22**, 555-558.

Murphy, W. F. III, k. W. Winkler, and R. L. Kleinberg, 1986, Acoustic relaxation in sedimentary rocks: Dependence on grain contacts and fluid saturation: Geophysics, **51**, 757-766.

Norris, A. N., 1985, A differential scheme for the effective moduli of composites: Mechanics of Materials, **4**, 1-16.

Nur, A., and J. D. Byerlee, 1971, An exact effective stress law for elastic deformation of rocks with fluids: Journal of Geophysical Research, **76**, 6414-6419.

Nur, A., G. Mavko, J. Dvorkin, and D. Galmodi, 1998, Critical porosity: A key to relating physical properties to porosity in rocks: The Leading Edge, **17**, 357-362.

Plona, T. J., and J. M. Cook, 1995, Effects of stress cycles on static and dynamic Young's moduli in Castlegate sandstone, *in* Procedings of the 35th U. S. Symposium on Rock Mechanics, J. J. K. Daemen and R. A. Schulz, eds., Balkema, 155-160.

Ragland, D. A., 2002, Trends in cementation exponents (m) for carbonate pore systems: Petrophysics, **43**, 434-446.

Raiga-Clemenceau, J., 1977, The cementation exponent in the formation factor-porosity relation: the effect of permeability: 18th Annual Logging Symposium, Society of Professional Well Log Analysts, Paper R.

Reuss, A., 1929, Berechnung der Fliessgrenze von Mischkristallen auf Grund der Plastizitätsbedingungen für Einkristalle: Zeitschrift für angewandte mathematic und mechanik, **9**, 49-58.

Risnes, R., and O. Flaageng, 1999, Mechanical properties of chalk with emphasis on chalk-fluid interactions and micromechanical aspects: Oil & Gas Science and Technologi, **54**, 751-758.

Røgen, B., L. Gommesen, and I. L. Fabricius, 2004, Methods of velocity prediction tested for North Sea chalk: a review of fluid substitution and v_s estimates: Journal of Petroleum Science and Engineering, **45**, 129-139.

Røgen, B., I.L. Fabricius, P. Japsen, C. Høier, G. Mavko, and J. M. Pedersen, 2005, Ultrasonic velocities of North Sea chalk samples: influence of porosity, fluid and texture: Geophysical Prospecting, **53**, 481-496.

Saha, S., G. B. Asquith, and L. Drager, 1993, A new approach to estimating S_w in carbonate reservoirs: The Log Analyst, **May June 1993**, 20-25.

Schön, J. H., 1996, Physical properties of rocks fundamentals and principles of petrophysics: Pergamon.

Shang, B. Z., J. G. Hamman, and D. H. Caldwell, 2005, Relating elastic and electrical properties via an equivalent rock element model: EAGE 67th Conference and Exhibition, European Association of Geoscientists & Engineers, H039.

Simmons, G., and W. F. Brace, 1965, Comparison of static and dynamic measurements of compressibility of Rocks: Journal of Geophysical Research, **70**, 5649-5656.

Solymar, M., 2002, Influence of composition and pore geometry on immiscible fluid flow through greensands: Ph.D. dissertation, Chalmers University of Technology.

Spencer, J. W, 1981, Stress relaxations at low frequencies in fluid-saturated rocks: Attenuation and modulus dispersion: Journal of Geophysical Research, **86**, 1803-1812.

Terzaghi, K. van, 1923, Die berechnung der Durchassigkeitsziffer des tones aus dem verlauf der hydrodynamischen spannungserscheinungen, Sitzungsber. Akad. Wiss. Wein Math Naturwissl Kl. Abt. 132, 105.

Tutuncu, A. N., and M. M. Sharma, 1992, Relating Static and ultrasonic laboratory measurements to acoustic log measurements in tight gas sands: 67th Annual Technical Conference and Exhibition, Society of Petroleum Engineers, 299-311.

Tutuncu, A. N., A. L. Podio, and M. M. Sharma, 1994, Strain amplitude and stress dependence of static moduli in sandstones and limestones: *in* P. P. Nelson and S. E. Laubach., eds., Rock mechanics- Models and Measurements Challenges from Industry, Balkema, 489-496.

Tutuncu, A. N., A. L. Podio, and M. M. Sharma, 1998a, Nonlinear viscoelastic behavior of sedimentary rocks, Part I: Effect of frequency and strain amplitude: Geophysics, **63**, 184-194.

Voigt, W., 1910, Lehrbuch der Kirstallphysik: B. G. Teubner-Verlag.

Walton, K., 1987, The effective elastic moduli of a random packing of spheres: Journal of Mechanics and Physics Solids, **35**, 213-226.

Wang, Z., 2000, Dynamic versus static elastic properties of reservoir rocks, *in* Z. Wang, and A. Nur, eds., Seismic and acoustic velocities in reservoir rocks volume 3 Recent developments, Geophysics reprint series No.19, 531-539.

Wang, Z., and A. Nur, 1988, Velocity dispersion and the “local flow” mechanism in rocks: 58th Annual International Meeting, SEG, Expanded Abstracts, 548-550.

Wang, Z., and A. Nur, 1990, Dispersion analysis of acoustic velocities in rocks: Journal of the Acoustical Society of America, **87**, 2384-2395.

Wang, Z, and A. Nur, 1992, Elastic wave velocities in porous media: A theoretical recipe, *in* Z. Wang, and A. Nur, eds., Seismic and acoustic velocities in reservoir rocks volume 2, Theoretical and model studies, Geophysics reprint series No. 10, 1-35.

Winkler, K. W., 1983, Contact stiffness in granular porous materials: comparison between theory and experiment: Geophysical Research Letters, **10**, 1073-1076.

Winkler, K. W., 1983, Frequency dependent ultrasonic properties of high-porosity sandstone: Journal of Geophysical Research, **88**, 9493-9499.

Winkler, K. W., 1985, Dispersion analysis of velocity and attenuation in Berea sandstone: Journal of Geophysical Research, **90**, 6793-6800.

Winkler, K. W., 1986, Estimates of velocity dispersion between seismic and ultrasonic frequencies: Geophysics, **51**, 183-189.

Wu, T. T., 1966, The effect of inclusion shape on the elastic moduli of a two-phase material: International Journal of Solids and Structures, **2**, 1-8.

Wyllie, M. R. J., and A. R. Gregory, 1953, Formations factors of unconsolidated porous media; influence of particle shape and effect of cementation: Transactions of the American Institute of Mining and Metallurgical Engineers, **198**, 103-110.

Yale, D. P., J. A. Nieto, and S. P. Austin, 1995, The effect of cementation on the static and dynamic mechanical properties of the Rotliegendes sandstone, *in* Procedings of the 35th U. S. Symposium on Rock Mechanics, J. J. K. Daemen and R. A. Schulz, eds., Balkema, 169-175.

Yale, D. P., and W. H. jr. Jamieson, 1994, Static and dynamic rock mechanical properties in the Hugoton and Panoma fields, Kansas: SPE Mid-Continent Gas Symposium, SPE, 209-219.

Zhanxiang, H., W. Dong, and Y. Lei, 2007, Joint processing and integrated interpretation of EM and seismic data- an effective method for detecting complicated reservoir targets: The Leading Edge, **March**, 336-340.

Zimmerman, R. W., 1991, Compressibility of sandstones: Elsevier.

The papers are not included in this www-version but can be obtained from the library at the Institute of Environment and Resources, Bygningstorvet, Building 115, Technical University of Denmark Dk-2800 Kgs. Lyngby, (library@er.dtu.dk).

Enclosure 1

Manuscript 1

Olsen, C., K. Hedegaard, I.L. Fabricius, and M. Prasad, Prediction of Biot's coefficient from rock physical modeling of North Sea chalk: Submitted to Geophysics.

Enclosure 2

Manuscript 2

Olsen, C., H.F. Christensen, and I.L. Fabricius, Static and dynamic Young's modulus of chalk from the North Sea: Submitted to Geophysics.

Enclosure 3

Manuscript 3

Olsen, C., T. Hongdul, and I. L. Fabricius, Prediction of Archie's cementation factor from specific surface or from porosity and permeability: Submitted to Geophysics.

Enclosure 4

Conference abstract

Olsen, C., I. L. Fabricius, A. Krogsbøll, M. Prasad, 2004, Static and Dynamic Young's Modulus of Marly Chalk from the North Sea: 66th Conference and Exhibition, EAGE.

Enclosure 5

Conference abstract

Olsen, C., I. L. Fabricius, A. Krogsbøll, M. Prasad, 2004, Static and dynamic Young's Modulus for Lower Cretaceous chalk. A low frequency scenario: International Conference and Exhibition, AAPG.

Enclosure 6

Conference abstract

Olsen, C., K. Hedegaard, I. L. Fabricius, M. Prasad, 2005, Modelling elastic moduli and cementation of North Sea chalk: 67th Conference & Exhibition, EAGE.

Enclosure 7

Conference abstract

Olsen, C., and I. L. Fabricius, 2006, Static and dynamic Young's modulus of North Sea chalk: 76th Annual International Meeting, SEG, Expanded abstract, 1918-1922.

Enclosure 8

Related study

Fabricius, I.L., C. Olsen, and M. Prasad, 2005, Log interpretation of marly chalk, the lower Cretaceous Valdemar field Danish North Sea: Application of iso-frame and pseudo water-film concepts: The Leading Edge, **May 2005**, 496-505.

Enclosure 9

Related study

Prasad, M., I.L. Fabricius, and C. Olsen, 2005, Rock physics and statistical well log analysis in marly chalk: The Leading Edge, **May 2005**, 491-495.

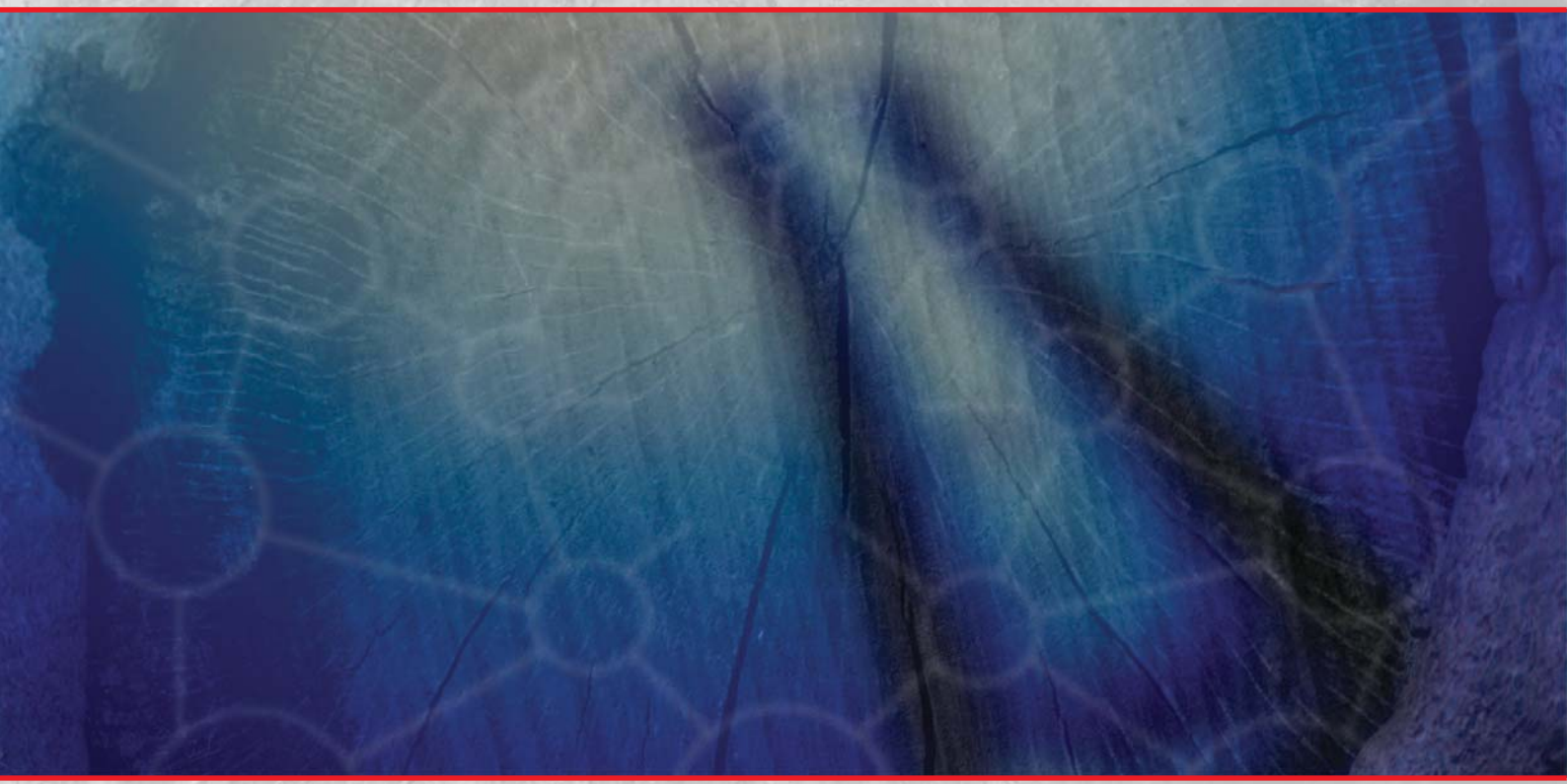

Institute of Environment & Resources
Technical University of Denmark
Bygningstorvet, Building 115
DK-2800 Kgs. Lyngby

Phone: +45 4525 1600
Fax: +45 4593 2850
e-mail: reception@er.dtu.dk

Please visit our website www.er.dtu.dk

ISBN 978-87-91855-41-2